The application of scanning electron microscopy to bulk devices I - Gunn diodes

University College of North Wales
Grant NGR-52-117-001

by

A. Gopinath, D.A. Shaw, D.V. Sulway and P.R. Thornton

School of Engineering Science
U.C.N.W., Dean Street,
Bangor, Caerns., U.K.

November, 1968.

N70-30429

THE APPLICATION OF SCANNING ELECTRON MICROSCOPY TO BULK DEVICES I - GUNN DIODES

A. Gopinath, et al.

School of Engineering Science
Bangor, Caerns, United Kingdom

November 1968

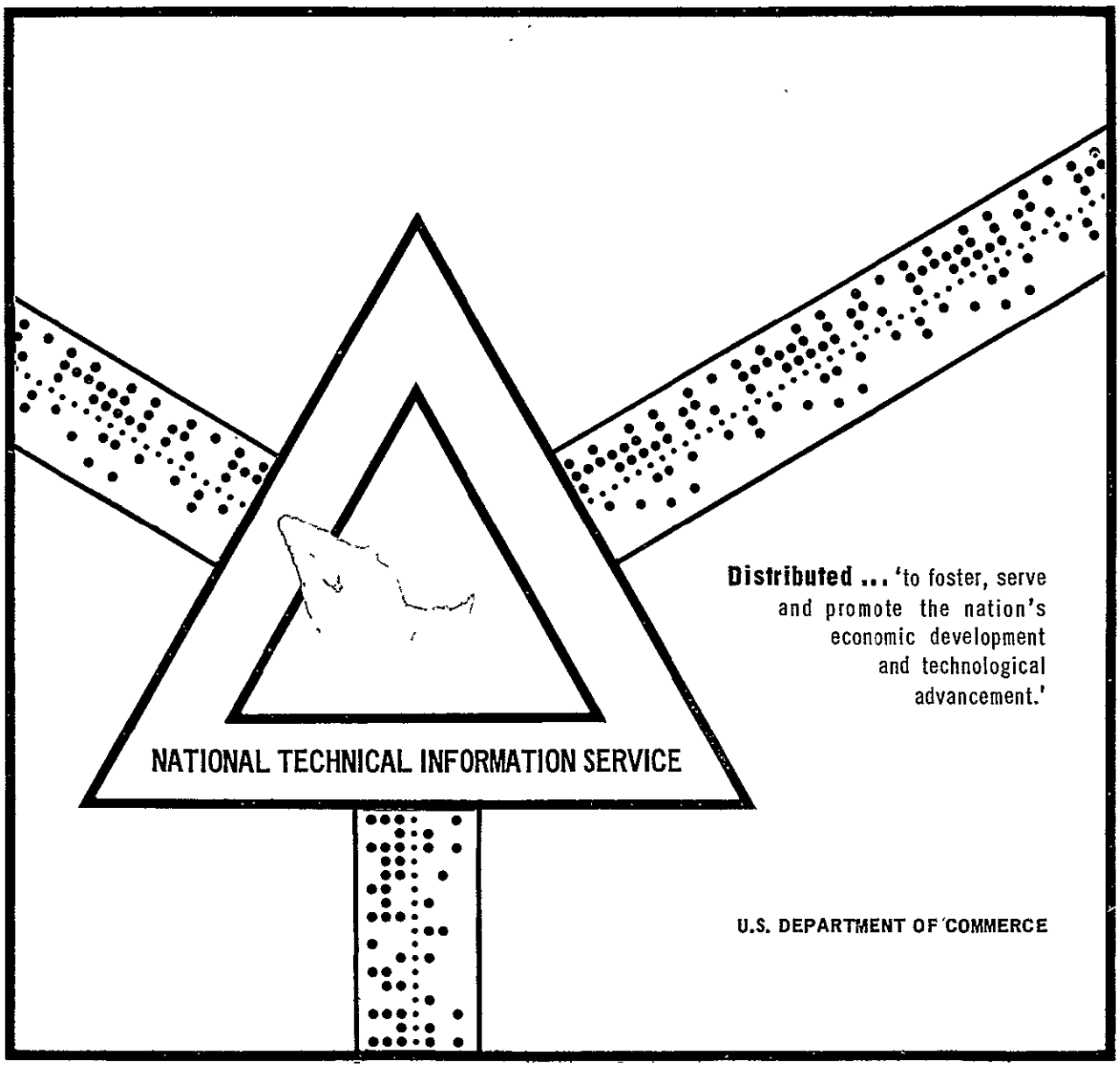

Application of scanning electron microscopy to bulk devices.

I - Gunn diodes.

I. Introduction (a) General

The object of the present contract is to investigate the methods whereby the application of scanning electron microscopy to device diagnostics may be extended. Hitherto the work has stressed, almost exclusively, junction devices. We were therefore interested in extending the approach to bulk devices. Munakata (1) has used an electron beam of relatively large diameter (12μ)to study the inhomogeneities in resistivity in bar specimens of size 1 mm x 1 mm x 1 cm. It is therefore of interest to investigate the possibilities of using a refined scanning electron beam to diagnose the properties of much smaller devices. In order to do this we accepted the invitation of Drs. Cyril Hilsum and Ian Bott of R.R.E. to examine the properties of small Gunn diodes made in epitaxiall grown GaAs. These devices have active lengths of the order of 10μ. We also used this investigation as a means of assessing the worth of a method of obtaining two dimensional quantitative data recently suggested by Flemming (2). The importance of this approach will become apparent below.

It was against this background that this work was undertaken. The following section outlines the problems associated with the experimental Gunn diodes that we sought to investigate. It should be stressed that these observations were obtained very recently and in order to include them in this report they have been described before they have been fully assessed and before the theory can be computed out.

2. Introduction (b) Behaviour of Gunn diodes made in epitaxially grown GaAs

The underlying ideas can be summed up by the following questions:-

(a) Is it possible to obtain information about the field distribution across the device in the low voltage regime before the onset of oscillations?

(b) Can experimental evidence be obtained of the way in which material inhomogeneities affect the device performance?

(c) Can any information be obtained about the temperature distribution in these devices as a function of wattage consumed?

(d) What suggestions can be made to increase the yield and performance of such devices and what light can be thrown on the failure and degradation processes occurring in these devices?

The devices made available were all made by epitaxially growing

GaAs onto a semi-insulating GaAs substrate. The chip size was approximately 500' square and the n-type epitaxy layer was about 5 : thick and was Cr-doped to .. 1 .. cm. Several device configurations were used all with alloyed Au contacts. One type consisted of two parallel Au evaporated strips separated by GaAs strips of widths varying between 10 and 15 μ. These devices were bonded to TO5 headers and the Au strips thermal bonded to the header pins. These devices were supplied in two forms -- some were supplied complete and others were supplied which had been cleaved half-way along the active area so that the field distribution at right angles to the surface could be studied. Another type of device was related to these strip diodes in that the structure was the same except that the contactsconsisted of two shallow 'vee' s' with the apices pointing towards each other. Thus the field increases towards the device centre. The angle of 'vee' s' was varied. The final device structure used was circular with a circular centre contact and an outer annular ring separated by an annular ring of GaAs between 10 - 25 μ wide. Micrographs are given later which show each of structures in detail.

3. Experimental methods

(a) Determination of field distribution

The extreme smallness of these devices precludes all the

standard methods of determining the required voltage distribution, with the possible exception of an ultra-refined tungsten probe method which is very time consuming, tends to be destructive and is limited in scope as only with prohibitive labour can two dimensional information be obtained on this scale. The conclusion is reached that a contactless method based on a scanning light or electron beam is necessary. Of these an electron beam is preferred because of increased resolution and increased ease of scanning provided it does not damage the specimen.

With an electron beam we have, in principle, two choices of experimental method to determine the required voltage distribution. One method exploits the well established voltage contrast mechanism (3) and the other approach uses the electron beam as a refined travelling light spot i.e. as a moving source of injected minority carriers. We chose the latter approach for the following reasons:

(1) The use of the voltage contrast mechanism in bulk specimens requires an extension of this technique which has been more often applied to junction devices. Whereas Munakata (1) has already established the value of the second approach for large specimens.

(2) The secondary electrons exploited in the voltage contrast mechanisms come from a surface layer only 100 to 500Å thick. Thus this method gives only an indication of the surface voltage which may be

significantly different from the voltage distribution at depths of 4 to 10 below the surface. It is this latter distribution that is required.

(3) The signal to noise ratio is better in the second method than in the first. Therefore the second method is more easily extended to quantitative studies based on a 'contouring' system. See below.

(4) The use of an electron beam to generate a 'photovoltage' across the specimen measures the local field directly and, within the limitations of the analysis used to interpret the data, can be made more accurate than a method based on the direct measurement of voltage.

The physical basis of the method is illustrated in figure 1 for the case of a uniform bar specimen. The specimen bias is supplied from a constant current source while the electron beam at a distance x_o from the anode injects an equal number of majority and minority carriers and so alters the local conductance in a volume near to the point of impact of the beam. As this change in conductance introduces a finite change in the resistance of the specimen a voltage change $\Delta V(x)$ appears across the specimen as a result of the beam excitation under constant current conditions. In order to calculate $\Delta V(x)$ under a given excitation we have to make a simplified model. We shall show later that the simplifications

made affect only tbe constant of proportionality relating the experimentally determined quantity and the required variable - the local field, E(x).

When the electron beam injects minority carriers into a region of the order of the beam diameter, continuity of the holes (in the case of interest here) is maintained by normal diffusion sideways across the specimen in the y-direction and downwards into the specimen in the z-direction whereas the motion of holes along the specimen length is by 'downhill-diffusion' towards the cathode and by 'uphill diffusion' towards the anode. In order to analyse this situation we make the assumption that the beam excitation maintains a steady state in which a layer of thickness equal to twice the diffusion length has its conductivity changed in a manner which is uniform in the y-direction and that the conductivity of the volume of the specimen outside this layer remains unchanged and just effectively acts as a shunt resistor in parallel to the modified layer. On this model we have a one dimensional flow equation to solve and determine the total change in specimen resistance $\Delta r(x_o)$. In terms of the parameters defined in figure 1(a) $\Delta V(x_o)$ is given by

$$\Delta V(x_o) = R_b \, \Delta r(x_o) V_S / \; R(R_b + R) \qquad \text{eq. 1}$$

where R_b is the shunt resistance of the bulk specimen, R is the resistance of the bombarded strip in the unperturbed case, while $R - \Delta r(x_o)$ is the corresponding resistance in the irradiated case, and V_S is the voltage applied across the specimen.

It remains to estimate $\Delta r(x_o)$.

3(b) Calculation of $\Delta r(x_o)$

We assume a steady state situation under the electron beam excitation. This assumption is equivalent to assuming that the movement of the beam during the time taken for a minority carrier to travel the length of the specimen is small. To establish the underlying ideas we shall examine the case where the electrical field is uniform along the specimen and the contacts are ohmic. In the high field case where diffusion (as opposed to drift) can be neglected, the equation to be solved is

$$E_x \mu_h \frac{d\Delta p(x)}{dx} + \frac{\Delta p(x)}{\tau_p} = 0 \qquad \text{eq. 2}$$

$$\text{for } 0 \ll x \lesssim L - x_o$$

where x_o is the position of the beam from the anode. On integration equation 2 gives

$$\Delta p(x) = \Delta p(x_o) e^{-x/L_D} + \text{constant} \qquad \text{eq. 3}$$

where $L_D = E_x \mu_n \tau_p$.

With the assumption that $\Delta p(L - x_o) = 0$ we obtain

$$\Delta p(x) = \Delta p(x_o)(e^{-x/L_D} - e^{-(L - x_o)/L_D}) \qquad \text{eq. 4}$$

$\Delta p(x_o)$ can, in principle, be found by equating the total increase in carrier pairs in the device to the rate of delivery of energy by the electron beam.

The increase in p(x) will increase the total conductivity by

$$\Delta \sigma(x) = q\Delta p(x)\,(1 + b)\mu_h \qquad \text{eq. 5}$$

and the total change in resistance will be

$$\Delta r(x_o) = -\int_0^{L - x_o} \frac{\Delta\sigma(x)dx}{\sigma^2 A_o} \qquad \text{eq. 6}$$

$$= \frac{-q(1 + b)\mu_h \Delta p(x_o)}{\sigma^2 A_o} \int_0^{L - x_o} (e^{-x/L_D} - e^{-(L-x_o)/L_D})dx$$

$$= \frac{q(1 + b)\mu_h \Delta p(x_o) L_D}{{}^2 A_o} \left[e^{-(L-x_o)/L_D} \frac{(L_D + L - x_o)}{L_D} - 1 \right]$$

$$= \frac{q(1+b)\mu_h \Delta p(x_o) L_D}{A_o} \cdot f\left(\frac{x_o}{L} \cdot \frac{L_D}{L}\right)$$

With the further assumption that the current density is constant we obtain from equations 1 and 6

$$\Delta V(x_o) = \frac{R_b V_S}{R(R_b+R)} \cdot q \frac{(1+b)\mu_h \Delta p(x_o) L_D}{J^2 A_o} E^2 f\left(\frac{x_o}{L} \cdot \frac{L_D}{L}\right) \quad \text{eq. 7}$$

The observed signal is therefore proportional to E^2 and to a function, f, which is dependent on beam position. The variation of $f(\frac{x_o}{L}, \frac{L_D}{L})$ depends significantly on $\frac{L_D}{L}$ and on beam position. If therefore L_D is known f can be determined and a relative measure of E^2 as a function of x_o found from $\Delta V(x_o)/f$. This process is valid only if E is a slowly varying function of x. If E varies too rapidly this variation has to be taken into account in equation 2 which, then, has to be resolved. There are other approximations inherent in the above analysis which can, however, be removed by the use of a computer. The point that the simple approach outlined above makes is that variations in the observed signal are not necessarily due to changes in the local electric field which can only be determined after some computation but even in the absence of a full analysis the observed behaviour is a very useful guide to device performance. See section 4.

3(c) Experimental methods - quantitative studies

The actual experimental method we use to exploit the interactions described in the previous sections has to meet two specifications. First it must provide an overall two dimensional 'picture' of the required information over the active area of the device and secondly it must enable us to take quantitative measurements along any line or across any area shown to be of significance. The best method for combining the two dimensional pictorial aspect of the data and the ability to extend to quantitative observations is the contouring system described by Flemming (2). The basis of this method is shown in figure 2. The two horizontal arrows represent the working range of the system (the effective range of the film used for example) from the viewpoint of the input signal. An input signal which is much bigger than the working range is fed to a circuit which contains two threshold detectors. The upper one is set at a level U and the lower is set at a value L. A logic circuit notes and stores every time the signal moves outside the range UL. The information is used to generate the digital version of the signal as shown in figure 2(b). This digital signal is fed back to the input in antiphase with the signal. So the nett effect as far as the output circuit

is concerned is that the signal is 'folded-back' on itself whenever it moves outside the range UL, see figure 2(c). In practice this means on the film that considerable enhancement of signal results and the micrograph is covered with a series of contours representing successive constant increments of signal while still retaining sufficient of the pictorial aspect for us to relate the signal immediately to the device structure. This is the method used here. The beam induced voltage change is fed to such a circuit and used to produce contoured micrographs as required, as a function of bias, magnification etc. The circuit used to form this display (and others) is given in Appendix A, both in outline and in detail.

3(d) Other experimental methods

The contouring studies outlined above were augmented with the following techniques:-

(1) The SEM was used in the emissive mode to obtain normal micrographs of the specimen surface.

(2) Since GaAs is a luminescent material studies of the localised variations in cathodoluminescent efficiency can be made to give information about the presence of material inhomogeneities. In addition, because the efficiency of the radiative processes are temperature dependent, such

studies can give indications of temperature effects.

(3) An infra red microscope was used to obtain direct estimates of the device temperature distribution. This instrument was used to obtain measurements of the total radiance from given areas which were used to give indications of the relative temperature distribution.

(4) A sampling system was used to determine the thermal response of these devices. The device bias was pulsed at a suitable duty cycle and a sampling system used to form a line scan or a micrograph of the signal at a given time after the application of the pulse. By varying the delay between the onset of the pulse and the sampling interval it is possible to watch the change of signal due to device heating.

4. Experimental results

4(a) Strip specimens, field distribution

Micrograph 1* introduces the results obtained on the strip specimens. Micrograph 1(a) is an emissive micrograph of the surface of device number PTD 18(2)a. The distance between the black arrow heads is 10 in this case. One point should be stressed about this structure. The Au wire bonds approach from the header pins from the top right of the micrograph and terminate at the bottom left. The end

*Owing to the close-down of the group the photographs for this report had to be prepared before the report was written, hence the numbering of figures is a little arbitrary. Each montage of micrographs is labelled by a number in a black circle. This is the number referred to in the text.

of one bond can be seen in the figure. We shall see later that this asymmetry in bond structure probably affects the temperature distribution in the device. Micrograph 1(b) is a beam induced current micrograph (a conductive micrograph) of the same device taken with a small bias on the specimen. This micrograph has not reproduced well and detail has been lost. But, even on the original which was taken well within the working range of the film, it was difficult to detect variations in signal along the active length of the device. This situation is to be contrasted with the micrographs 1(c) to 1(f) which are contoured conductive micrographs of the same device taken at a function of bias. Consider the sequence 1(c) to 1(e) first. It is apparent that there are variations along the specimens and that these variations increase in magnitude as the bias is increased, but they do not change in character, i. e. the peaks and troughs remain in essentially the same positions. (Note:- the apparent signal from parts of the device outside the active area arise because these parts scatter primary electrons into the active area). We shall consider the origin of these variations later but we can point out one cause from this sequence of micrographs. Consider micrograph 1(a). To the immediate right of the lower arrow head and about " to the left of this arrow the Au contact has been 'smeared' across part of the

active area. These irregularities in contact structure affect the field distribution. See micrographs 1(c) to (e).

It can be seen from micrograph 1(f) that the field distribution has changed in character. The distribution in the centre of the device does not change in character but the region at the left hand end (indicated by the white arrow) has changed. We shall see later that this change is associated with a temperature increase in this region.

Micrograph 2 is a sequence of micrographs taken of a device (number PTD 18(2)) which was free from contact faults. This sequence shows that the observed pattern is dependent on the direction of the applied bias. Micrographs 2(a) to (f) is a sequence of conductive micrographs taken at the biases shown in the figure caption with the right-hand contact earthed and the left-hand contact at a positive potential. With the exception of the apparently gross irregularities at the bottom of the device which are caused by the presence of dust particles (see surface micrograph at the start of the sequence), the signal is reasonably uniform with only minor irregularities. If the bias direction is reversed the observed signal is more uniform. This result can be seen by comparing micrographs 2(g) and (h) with micrographs 2(c) and (d). These pairs were taken under identical conditions except that the bias was reversed.

We believe that the variations in signal arise from the presence of small variations in the electrical properties of the starting material. The change in signal resulting from these variations depends on the position of the variations relative to the cathode and so depends on the direction of the bias. It is also possible that the contacts have different field distributions associated with them and that the current flow under constant bias differs in the two directions. The following section also gives an indication of a possible cause of the anisotropy in current flow.

4(b) Strip specimens- effects due to temperature variations

Micrograph 5 contains observations of the device shown in micrograph 1. One initial point should be noted about this micrograph. Some of the micrographs do not agree in detail with those shown in the earlier micrograph. It should be remembered that this method of recording the signal is very sensitive. Small changes in the input gain setting can move the actual contours recorded a considerable distance across the active area while still recording the same information. Although this is a contributary cause of the differences observed, the main cause is the fact that the series shown in micrograph 3 was obtained

after the device had been examined in the SEM and in the infra-red microscope for considerable periods often under high biases or at high temperatures and had become degraded in the sense that its properties had been permanently changed. This degradation does not affect the content of this section because the region we are concerned with is outside the active area as defined by the contacts. Consider micrograph 3(b). At the bottom of the device, below the left hand contact there is a diffuse line which is indicated by the head of the white arrow. With the bias in one sense this region did not appear to change significantly as the bias was increased. See the sequence of micrographs 3(b) to (e). With the bias in the opposite sense this region gives a signal comparable in strength with that from the active area at high bias values. This increase in signal can just be seen from the sequence of micrographs 3(f) to (i), where a black signal (indicated by the arrow) can be seen in micrograph 3(i). This region was examined in more detail. The results are shown in micrograph 4. Micrographs 4(c) to (f) show the behaviour of this region as a function of voltage. By careful examination of the surface it was possible to locate a contrast feature on the surface associated with this region. Micrograph 4(a) was taken under normal contrast

conditions and the surface marking is only just discernable at the at the arrow head. In the following micrograph it is revealed with ease by using high contrast conditions. We shall see in a later section dealing with annular diodes that the material from which these diodes were made conclude regions of differing resistivity. So it is likely that this region shown in micrograph 4 is a high current path. If this is the case it is likely that a local temperature rise occurs because of the associated Joule heating.

By means of infra red microscopy we showed that there is a temperature increase associated with this area. Micrograph 5(b) is an infra-red micrograph of this area taken with the device in air at 10 volts bias. The numbers on the contours are arbitrary but are monotonic with temperature in degrees centigrade. Bearing in mind the fact that the optics used integrated the emitted radiance over an area 10 in diameter, it is likely that the 'temperature' at the 'core' of the high current region is considerably higher than indicated here.

Micrograph 5(a) is an infra-red map of another device. In this case the contour figures indicate the relative values of the emitted radiance not the temperature. We believe it is significant that the 'hot spot' again occurs at the end away from the header pins. We suggest

that the Au wire plays a significant role in cooling the device. It is the absence of heat conduction at the end with terminated wires that causes the temperature to increase at this end.

4(c) Angled specimens - field distributions

Micrograph 6 shows a sequence of micrographs of an angled device in which the degree of angling is relatively slight. Micrographs 6(a) and (b) show the surface of the device used. The remaining micrographs are contoured conductive micrographs taken as a function of bias. Three points emerge as a result of these studies. The first point concerns the high degree of symmetry observed on these diodes over the whole voltage range used and for both directions of bias. Some of the micrographs shown have up to 10 contours. Even if one contour were completely missing from one side of the device compared to the other then the variations in material properties leading to the signal would only be of the order of 10%. The fact that the comparative contours are only displaced by a few microns on the device imply that the materials variations are of the order of 1 to 2%.

The second point of interest concerns the behaviour of the signal, i. e. the contours, at the apex of the angle. Over the whole voltage

range employed, with the possible exception of the very highest voltage used, the contours are 'forced' away from the contact. This reduction in signal close to the apex appears at both anode and cathode to about equal extents for both signs of bias. At present we have no explanation of this effect. It was not observed on an angled diode in which the 'angling' was sharper (see below).

Finally, we observed from micrograph 6(k) that there is a 'stray' field signal from outside the contacts.

Micrograph 7 shows higher magnification contoured micrographs of another angled device with sharper apices. Again the high symmetry of the pattern is evident and provides further support for the contention that the material from which these devices were made is very uniform. In this device there is no 'forcing' of the contours away from the apices as was the case for the device examined in micrograph 6.

One experimental point that has to be checked in such studies as these is whether the results observed are representative of the 'bulk' of the device and not affected by purely surface effects. The devices studied are intended for use as Gunn oscillators. It is

probable that the volume of the crystal exploited in this application extends in depth from 1μ down to 10μ. There are two methods of determining if surface effects are contributing to the observed signal. One method is to vary the depth of penetration of the electron beam and observe the way in which the signal varies. The second method is to subject the device to various treatments to alter the surface properties and examine the effect on the observed signal. Micrograph 8 shows results obtained by using the first approach. At beam voltages of 5kV and less (corresponding to penetration depths of 2,000Å or less) there are changes in the geometry of the signal. The distribution tends to become more symmetrical, instead of peaked towards the anode. However, at beam voltages of 10kV or greater (penetration distances $> 1\mu$) the signal varies little with depth and has the characteristics predicted by theory. In view of of this result it is probably adequate to regard the signal distribution obtained with a 15kV beam as representative of the bulk of the device.

4(d) Annular devices - initial results

In contrast to the results obtained with angled devices the behaviour of the annular devices is very variable. Micrograph 9 shows the

behaviour of a good device. The signal has the circular symmetry of the device geometry. The main deviations from circular symmetry are small and are caused either by the central bond, or by surface markings. Only one asymmetric region unrelated to trivial faults can be observed and this is the region to be seen at '8 o'clock' in micrographs 9(f) and (i). The exact significance of the spacing between the contours with the two directions of bias will not be apparent until we have analysed the signal for this particular geometry.

Micrograph 10 shows another annular device which has a gross material fault extending nearly the whole way between the contacts. The fault is revealed by the conventional conductive micrograph 10(b). This fault affects the device behaviour drastically in both directions of bias. Micrograph 13 shows further observations on the same device. Micrograph 13(a) is a cathodoluminescent (CL) micrograph of this device taken at a beam voltage of 30kV. It is important to stress that this CL micrograph reveals all (and more) of the defects revealed by the conductive micrograph. Since a bond is not necessary to obtain CL micrographs this approach, it is suggested, should be used to assess the material prior to device fabrication. Micrographs 13(d) to (f) are contoured CL micrographs taken after the device had been subjected

to 6 volts bias in one sense for several minutes. While micrograph 13(f) is a similar micrograph taken after the bias had been applied in the opposite sense. In both cases the signal is reduced, in one micrograph obtained after heating one contour out of three is missing compared to the non heated specimen, in the other micrograph two contours are missing. This reduction in CL signal is most likely due to increase in specimen temperature.

Micrographs 13(b) and (c) are a conductive and emissive micrograph of the same area and show that most of the details revealed on the conductive micrographs are not apparent on the surface micrograph and so lie below the surface.

Micrographs 11 and 12 show similar studies of the third annular device studied. The comments made in the previous paragraphs are applicable and the only new points concern micrograph 11(b) and micrograph 12(a). The first of these shows the presence of material faults which are the cause of one of the major defects observed. The second of these micrographs illustrates irregularities in the central metal pad. These irregularities are associated with the second major defect observed.

4(e) Observations on cleaved specimens

Micrographs 14 to 16 show observations made on a cleaved device. The essential conclusions from these studies are (1) the interface between the semi-insulating substrate and the epitaxial layer can be revealed on the emissive micrographs (see 10(b) and (c)) ; (2) it is possible in practice to examine the field distribution in depth in this way to a good resolution (see micrograph 16); (3) careful consideration has to be given to the experimental design if this type of study is to be meaningfully interpretated. In particular we have to establish whether the very act of cleaving creates new boundary conditions and so alters the field distribution in such a way that it cannot be related to the distribution halfway along an operational device. It may be better to etch rectangular holes of varying depth in the active area and to examine the depth dependence of the signal in this way.

4(f) Observations of failure mechanisms

Micrograph 17 shows initial observations of failure areas. The first three micrographs showed areas in which failure has already occurred More importantly micrographs 17(d) and (e) show an incipient feature. There is no evidence of the would be failure on the surface (micrograph

17(d)). However an anomalous signal is seen developing on the left hand side of the device in the contoured conductive micrograph 17(e). Initially the 're-entrant' contours were only about 1 mm long but extended further after Joule heating. Usually, but not always, these permanent changes occur in regions with material faults.

4(g) Sampling techniques applied to the contouring system

We have completed feasibility studies in which a commercially available sampling system was used to investigate the signal from chosen areas at a selected time after the application of a pulsed bias. We were able to show that the thermal induced changes in signal could be followed from .2 S after the application of the pulse. At present instrumental difficulties limit the general application of the technique. In particular the sampling time on available systems is too small for this type of work and the scan generators available do not perform satisfactorily at the slow scan rates required. These difficulties should be easily overcome and we are seeking to extend these studies to examination of the field distribution over the range of voltages in which oscillations occur.

5. Discussion and Conclusions

We have already emphasised in an earlier section that this report

should be regarded as an initial write-up of a feasibility study. In particular we stressed that the quantitative interpretation of the signals needs further examination. On the credit side we have

(a) Established the worth of the contouring method of signal enhancement and of obtaining quantitative, two-dimensional information in a high resolution instrument.

(b) Shown the value of the method to bulk devices with small active areas.

(c) In particular we have shown

(1) how the symmetry of the observed signal can be used to assess the quality of the device;

(2) indications that the signal observed is characteristic of the volume of the device which is important in the operation of the device;

(3) how the CL can be exploited to assess the material prior to fabrication;

(4) how incipient failure processes can be studied;

(5) the feasibility of using sampling techniques in this type of problem;

(6) that it may be possible to improve the heat carrying ability of the devices by using thicker (or more) Au bonds.

With regard to the extension of this work, a computer study of the predicted signal variation in cases of interest is already under way, and plans are laid to extend the use of the sampling technique into the oscillating regime.

6. Acknowledgements

We should like to thank Dr. P. Flemming of S. T. L., Harlow for very full discussions of the contouring approach before publication.

References

1. C. Munakata, Journ. of Scientific Instr. 1, 639, (1968).

2. P. Flemming. To be published in Journ. of Scientific Instr.

3. C.W. Oatley and T. E. Everhart, J. Electronics, 2, 568, (1957).

APPENDIX ONE

Description of the Circuit and Operation of the Contour Display System

(1) Introduction

The system described below is a modified version of a circuit first devised by Flemming (1). This circuit is one way of obtaining two dimensional quantitative information quickly from scanning beam instruments with no loss of information. It was initially developed for use on a modified videocon which gives relatively low resolution, but has now been applied successfully to a high resolution scanning electron microscope.

(2) Description of Operation

The operation of the system is best understood with reference to the block diagram, Fig. 1. The signal of interest is applied to one input of the summing amplifier A, the gain being determined by the resistors R_1 and R_2. The output of the amplifier is applied to the two threshold detectors T_1 and T_2. T_1 will operate whenever the applied signal goes more positive than in the present case, + 1.5V, and T_2 whenever the signal goes more negative than - 1.5V. When a threshold detector is

triggered the output swings from negative saturation to positive saturation and, ignoring for the moment the box S, a count command is applied to the counter C. C is an up-down counter, the negative sensing threshold detector providing a count-down command and the positive one a count-up command. An analogue output of the state of the counter is provided by the D/A convertor and is fed back to the other input of the summing amplifier A. Let us now consider the case of a sine wave applied to the input, see Fig. 2.

If the input signal is at a positive going part of the cycle, the output of the amplifier will go more negative until the negative sensing theshold detector is triggered. This will make the counter count down one step and the change in level fed back to the input from the D/A convertor via R_3 will be such as to reduce the total input to the amplifier A so that the threshold detector turns off and the counter maintains its new state until one of the threshold detectors is again triggered. The size of the step fed back from the D/A convertor is such that the level at the output of the amplifier (O/P A) {falls / rises} from one threshold level to just {above / below} the other threshold level, as shown in Fig. 2, output A. The input signal continues to go more positive and again is returned almost to the lower threshold. The reverse process occurs on the negative going part of the cycle.

Using this system on a charge collection signal (or any other signal) derived from the scanning electron microscope and displaying the output (A) on a C.R.T. in the normal way, we observe a series of dark/light interfaces corresponding to the steps shown in Fig. 2. These interfaces form contours connecting points of equal signal amplitude, the normal amplitude modulated signal being displayed between these contour lines. Increasing signals and decreasing signals can be differentiated as in one case a light to dark transition will occur and in the other a dark to light transition.

The counter is synchronised to a clock, D, and will remain stationary unless the clock period is such that it can change its state. As the input signal is not synchronous with the clock, a count command from the threshold detectors can occur at any point during the clock pulse, even when the counter is unable to respond. For this reason a store or delay, S, is introduced between the threshold detectors and the counter so that a count command can be stored (for a maximum period of one clock pulse) until the counter can operate. The spatial error introduced by this delay is negligible, being typically of the order of 1,000Å. However, the presence of this store can lead to serious errors.

If a count up and a count down command occur in rapid succession (within one clock period), the store could contain both commands, which, if fed to the counter would lead to erroneous results. Under these conditions the gate, G, prevents the counter operating and the store is cleared. In addition to output A, which is the most important output containing all the available information, two others are provided. Output B (see Fig. 2) is derived from the outputs of the two threshold detectors via the adding unit P. This output gives a positive pulse when the positive threshold detector is triggered and a negative pulse when the negative detector operates. When displayed on a C.R.T. the pulses from contour lines of equal signal amplitude but with no information between the contours. Again, increasing and decreasing signals are differentiated by the sign of the pulses making up the contour. Output C (see Fig. 2) is derived from the D/A convertor and is a stepped reconstruction of the input signal, the width of the steps being the distance between contour lines. When displayed on a C.R.T. areas of different intensity 'greys' are produced corresponding to the areas between adjacent contour levels.

(3) The Circuit

A complete circuit diagram is shown in Figs. 3(a), (b) and (c). The input summing amplifier (Motorola MC1709C) is a conventional

configuration using switched input resistors to vary the input signal gain. Voltage gains of 10, 20, 50 and 100 are provided. The threshold detectors (Motorola MC1710) are also conventional circuits. The threshold levels are set to ± 1.5V although this can be varied by altering the scaling resistors at the inputs of these units. The zener diodes D_1 and D_2 provide the D.C. shift necessary as the logic '0' level is -12 volts. The 1K resistors following the zener diodes speed up the switch off time of the threshold detectors. The flip-flops F_1 and F_2 (Motorola MC790P) provide the delay or count command store whilst nor-gates G_1 and G_2 (Motorola MC724P) prevent simultaneous up and down commands. Flip-flops F_3 to F_9 constitute the up-down counter which is again a 'standard' circuit. Transistors Tr8 to Tr13 are the D/A circuits whilst transistors Tr1, 3, 4 and 5 provide the power supplies for these circuits. Transistors TR2, 6 and 7 provide an automatic 'zero' control. As the step size is altered the standing current in the collector circuit of Tr1 will vary possibly resulting in the saturation of the input summing amplifier. To prevent this an equal and opposite change in current is provided from the collector of Tr7. The current from Tr7 is such that with no signal input, the

counters are set midway up the count so that either positive or negative going signals can be accommodated. Transistors Tr14 and 15 are two simple switching circuits providing the added pulse output. Fig. 3(b) shows a suitable power supply circuit providing all the voltage supplies needed for the various sections of the circuit from ± 15V rails. The current drain is ~60mA from the +15 V rail and ~420mA from the -15V rail. Two nor gates were used in a multivibrator circuit to provide the clock generator giving a clock frequency of ~500 kc/s, see Fig. 3(b). The system is D.C. coupled and will thus respond to very slow changes of input level (however, see below). The speed of response of the system is such that with relatively noise-free signals (see below) a line scan speed of 1mSec can be used. The step size was adjusted so that the signal was stepped from one threshold level to just short of the other level (i. e. just short of oscillation). This gives the most symmetrical display and was found to be the most useful. It does present difficulties however, which are discussed below.

(4) Difficulties associated with the present system

Setting up the D/A convertor so that the steps are all equal was

found to be quite difficult using the present circuit, especially when a large number of contour levels was required. When only a small number of levels is required as is usual in practice (see earlier in this report) then the problem is not as serious. In order to make setting up easier, very constant voltage sources must supply both the scaled loads of the D/A stages and the dummy loads (1K). In the present circuit the supply for the dummy loads is not entirely satisfactory and the system would be improved if it were changed to the same type used for the scaled load supply. Another slight difficulty of the present system occurs when a signal approaches the threshold level very slowly or at a 'tangent'. Under these conditions the threshold detector will oscillate i. e. it will repeatedly switch on and then off. The effect is readily interpreted and so no real problem exists however, the oscillations could be cured by the addition of positive feedback to the threshold detectors. The addition of some hysteresis would also help but this would also increase the delay time possibly to an intolerable level. When dealing with very noisy signals as frequently happens, e. g. using the charge collection mode of the S. E. M. another problem arises. The noise peaks can trigger the threshold detectors and, although the

threshold level may only be exceeded for a very short time, if the clock period is such as to allow the counter to operate then erroneous results occur. With extremely noisy signals the noise can be so great that after triggering one threshold detector, the other detector is triggered and oscillation results. This problem has been solved by the use of filtering and phase sensitive detection and although slow line speeds must be used, extremely noisy signals have been dealt with successfuly (see earlier part of this report). This problem could also be solved by increasing the threshold levels and/or reducing the step size.

Another difficulty is associated with the use of output C from the D/A convertor. When using a number of contour levels the range of the output from C is such that it is difficult to accommodate all the grey levels needed on Polaroid film. Also, as the circuit stands at the moment, the output from the D/A convertor needs additional amplification.

Perhaps it should be noted here that none of the outputs from this unit will drive the video amplifier of the scanning electron microscope directly, a suitable buffer amplifier must be provided.

References

1. P. Flemming, J. Sci. Instrum. to be published.

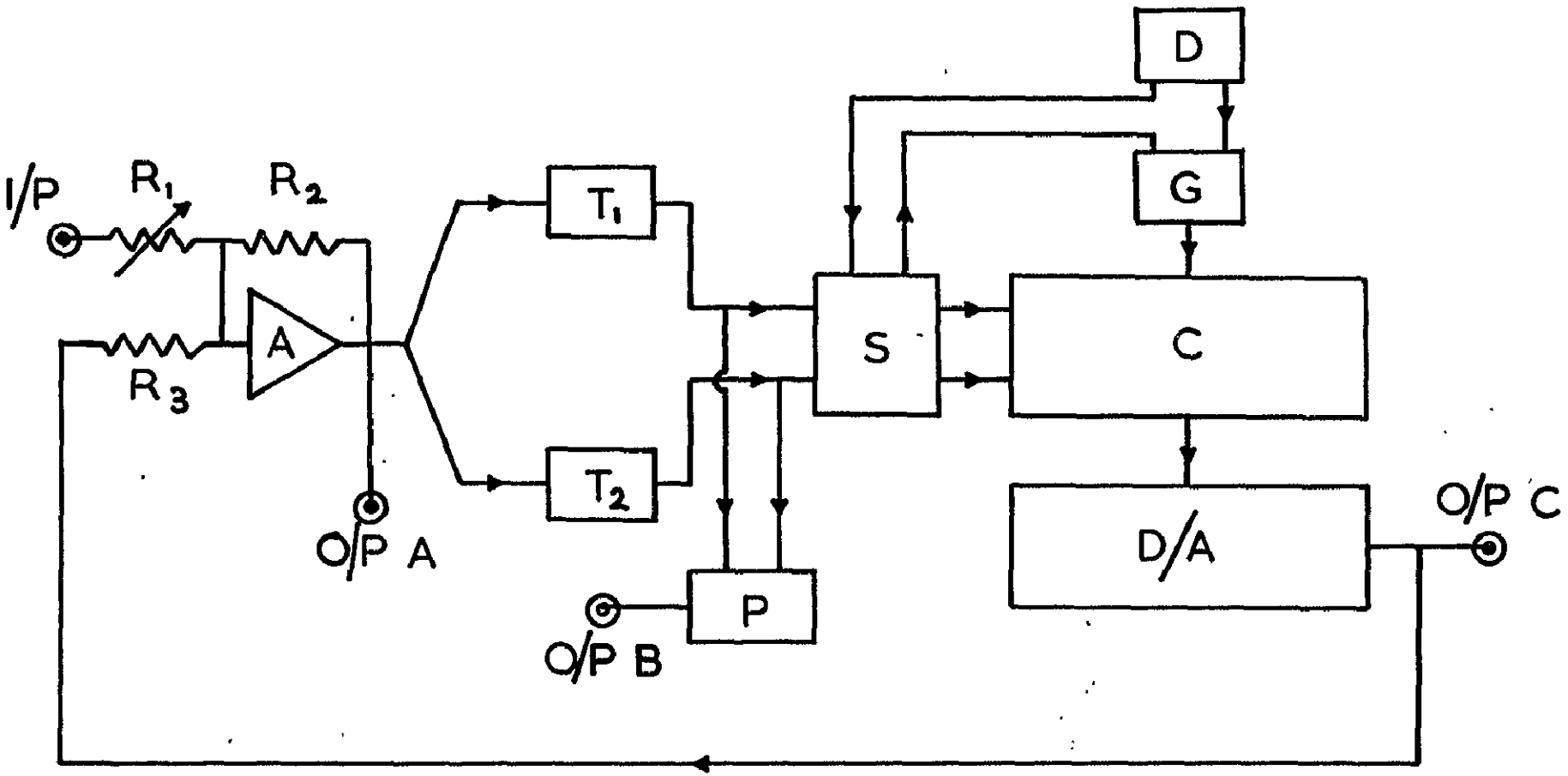

FIG. 1

FIG. 2

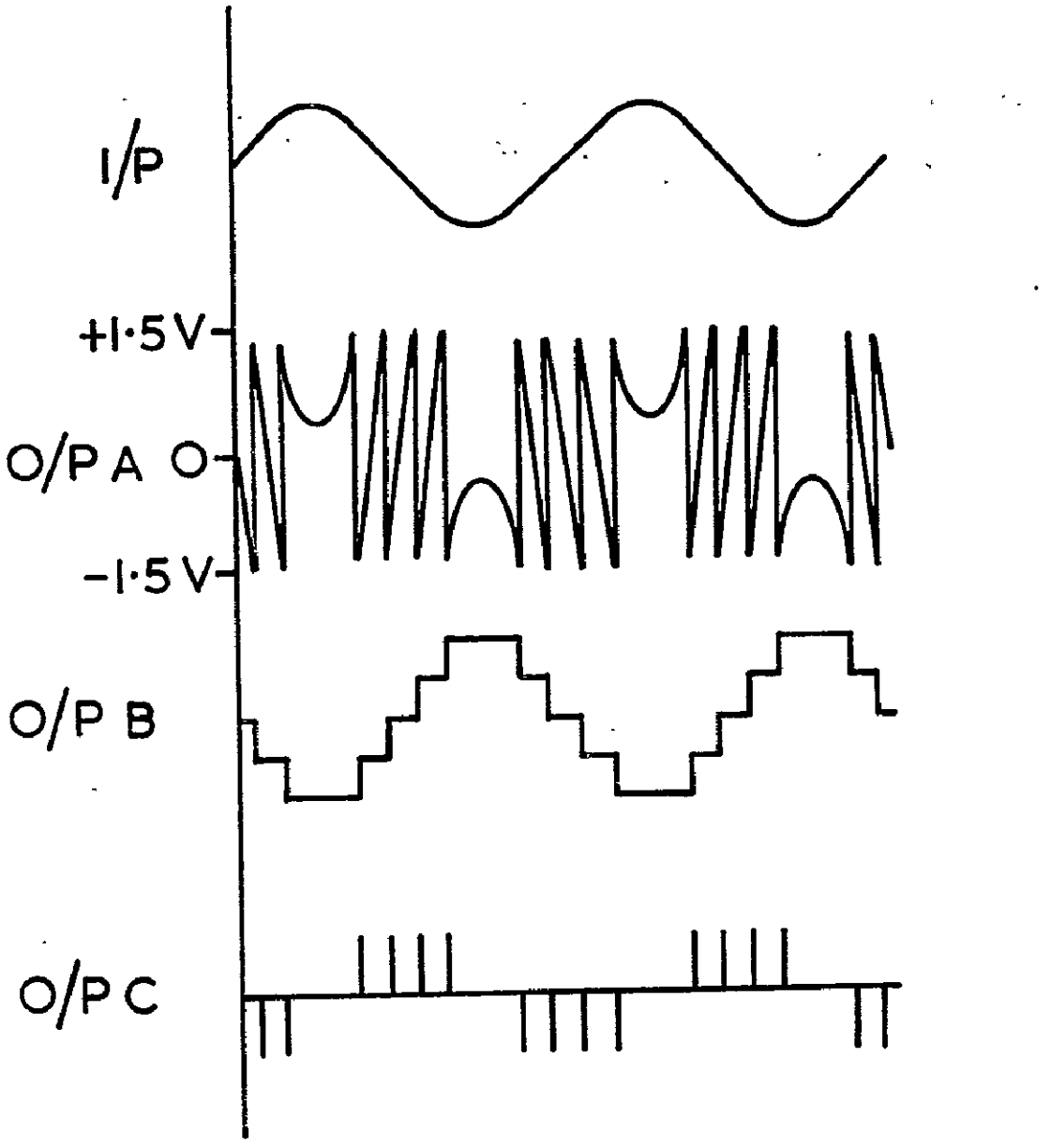

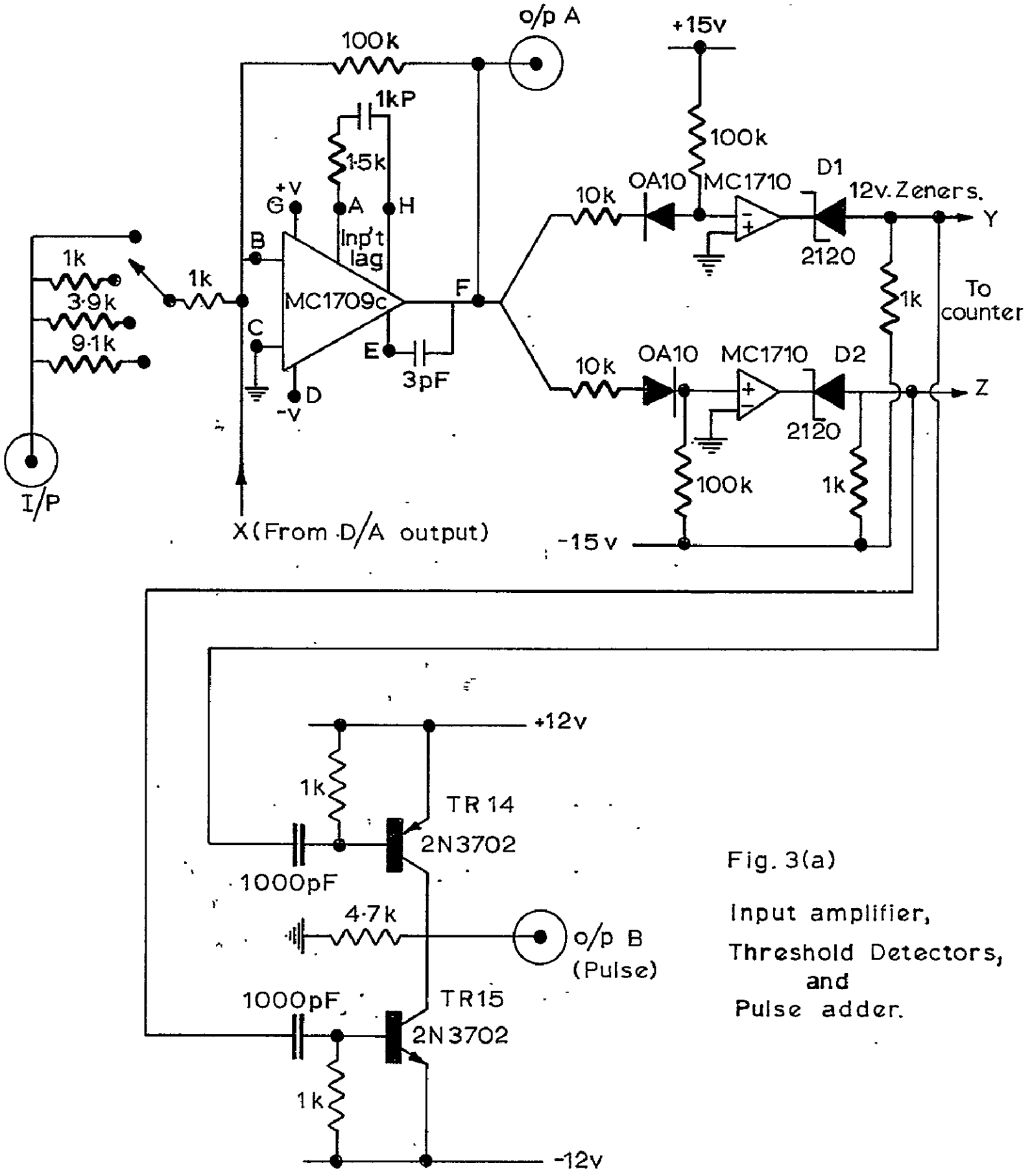

Fig. 3(a)

Input amplifier,
Threshold Detectors,
and
Pulse adder.

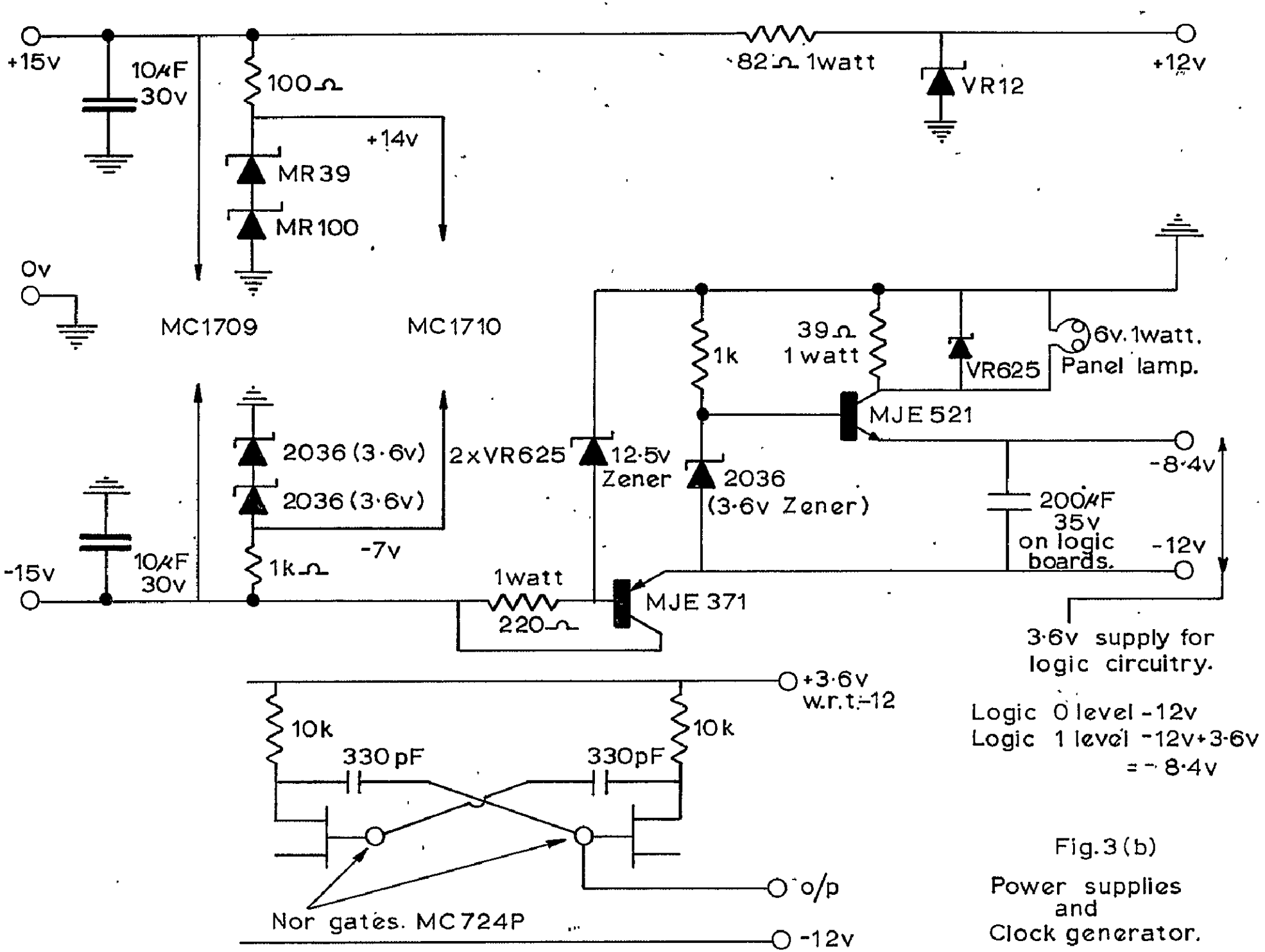

Fig.3(b)

Power supplies
and
Clock generator.

Captions to figures and micrographs

Figure 1. Definition of parameters used to analyse the conductive signal.

Figure 2. Physical basis of contour method.

Micrograph 1 Device number PTD 18(2)a, 110μ(a) emissive micrograph of surface; (b) normal conductive micrograph of device at bias indicated; (c) to (f) contoured conductive micrographs taken at the biasses indicated.

Micrograph 2 Device number PTD 18(2), 110μ, emissive micrograph followed by sequence of conductive micrographs taken at different biasses. Bias applied to left hand contact.
(a) = + .96 volts; (b) + 3.2V; (c) + 3.52V; (d) + 4.8V; (e) + 5.93V; (f) + 6.02V; (g) - 3.52V; (h) -4.8V.

Micrograph 3 Device number PTD 18(2), a 110μ, (a) emissive micrograph of surface, remainder is a sequence of conductive micrographs with the following biasses applied to the left hand contact:-
(b) - .1V; (c) - 1.0V; (d) - 3.0V; (e) - 6.0V; (f) + .1V; (g) + 1.0V; (h) + 3.0V; (i) +6.0V.

Micrograph 4 Device number PTD 18(2)a, 110μ(a) emissive micrograph of detail at bottom of left hand contact; (b) similar micrograph of same detail at higher contrast (c) to (f) conductive micrograph of same detail at voltages of + 3, + 4, + 5 and + 6 volts applied to the left hand contact respectively.

Micrograph 5 (a) Infra red map of device number PTD 18(2)c, 100μ. Figures on the contours indicate relative values of the emitted radiance. (b) Corresponding map of device number PTD 18(2)a, 110μ.

Micrograph 6

Device number PTD 17, 400μ. (a) and (b) emissive micrographs of the surface. (c) to (f) contoured micrographs taken with the following bias applied to the upper contact.
(c) + .11V; (d) - .12V
(e) + 1.02V; (f) - 1.01V
(g) + 3.04V; (h) - 3.02V
(i) + 6.02V; (j) - 6.10V
(k) which shows the field distribution outside the contacts was obtained with + 1.09V bias.

Micrograph 7

Device number PTD 17, 660μ; bias applied to left hand contact; beam voltage = 15kV.
(a) -.16 volts; (c) -1.0 volts; (e) -3.0 volts;
(g) - 6.0 volts; (i) -8.0 volts; (k) - 10 volts;
(b) + .17 volts; (d) + 1.0 volts; (f) + 3.0 volts;
(h) + 6.0 volts; (j) + 8.0 volts; (l) + 10 volts.

Micrograph 8

Device number PTD 17, 660μ, bias 6V negative applied to left hand contact, conductive micrographs taken as a function of beam voltage, (a) 25kV; (b) 10kV; (c) 5kV; (d) 3kV; (e) 2kV.

Micrograph 9

Device number PTD 14, Ring 2, 300 (a) emissive micrograph, (b) conductive line scans with +1, +3 and +6 volts applied to centre contact, (c) corresponding line scans with -1, -3 and -6 volts applied to centre contact (Note the peaks in the curves in (b) get higher as the bias is increased, whereas in (c) the peaks increase in the order 1, 6 and 3 volts); (d) to (i) contoured conductive micrographs taken with the following biases applied to the centre contact
(d) + .13V; (g) - .13V
(e) + 3.00V; (h) - 3.00V
(f) + 6.03V; (i) - 6.00V

Micrograph 10

Device number PTD 14, Ring 1, 333μ (a) emissive micrograph of device, (b) conventional conductive micrograph with .25 volts on centre contact, (c) to (j) contoured conductive micrographs taken with the following voltages on the centre contact.
(c) - .11V; (g) + .10V
(d) - 1.00V; (h) + .98V
(e) - 2.96V; (i) + 3.06V
(f) - 5.95V; (j) + 6.08V

Micrograph 11

Device number PTD 14, Ring 4, 300μ, (a) emissive micrograph of device, (b) corresponding contoured conductive micrograph (+ 1.03V on centre contact); (c) emissive micrograph of area studied in subsequent micrographs; (d) contoured conductive micrograph with +1.02 on centre contact before heating by increasing voltage to +6V; (f) similar micrograph with - 1.04V on centre contact; (g) similar micrograph with +6.06V on centre contact.

Micrograph 12

Device number PTD 14, Ring 4, 300μ, (a) emissive micrograph of device (b) to (h) contoured conductive micrographs taken with the following biasses applied to the centre contact.
(e) + .15V
(b) - 1.03V; (f) + .99V
(c) -2.95V; (g) + 3.02V
(d) - 5.95V; (h) + 6.08V

Micrograph 13

Device number PTD 14, Ring 1, 333μ(a) cathodoluminescence micrograph, (b) conductive micrograph of part of the device; (c) emissive micrograph of area corresponding to (b); (d) to (e) contoured cathodoluminescent micrograph taken with 0, - 5.95 and + 6.00 volts on centre contact respectively.

Micrograph 14

Device number PTD 18, 300μ(a) emissive micrograph under normal contrast conditions; (b) similar micrograph with increased contrast to expose edge of epitaxial layer; (c) magnified view of part of (b), (d), (e) and (f) contoured conductive micrographs taken with top two contacts shorted together and held at +1.00V, + 3.02V and +6.02V relative to earth and substrate respectively.

Micrograph 15 — Contoured micrographs of device number PTD 18, 300μ with bottom contact and substrate earthed and top contact at the following potentials
(a) - .14V; (e) + .14V
(b) - 1.00V; (f) + 1.00V
(c) - 3.00V; (g) + 3.00V
(d) - 6.01V; (h) + 6.10V

Micrograph 16 — Similar to micrograph 15 with following biasses
(a) - .11V; (c) + .12V
(b) - 1.00V; (f) + 1.00V
(c) - 3.00V; (g) + 3.04V
(d) - 6.00V; (h) + 6.04V

Micrograph 17 — Failure mechanisms in Gunn diode. (a) Surface topograph of failed device; (b) magnified view of failed area; (c) view of region which shows successive multiple failures; (d) and (e) region of incipient failure; (d) shows unperturbed surface; (e) shows contoured conductive micrograph of underlying incipient failure.

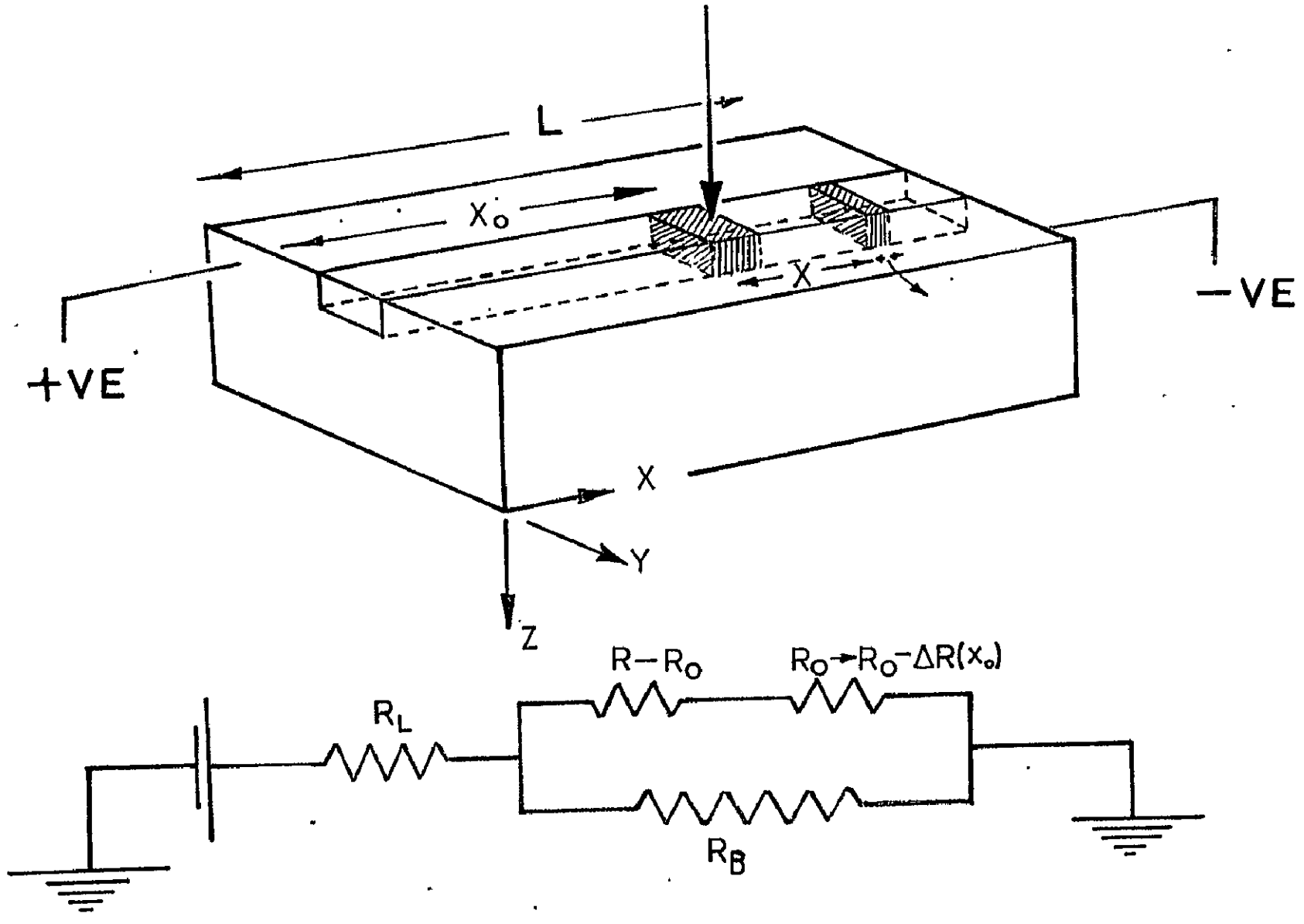

FIGURE.1.

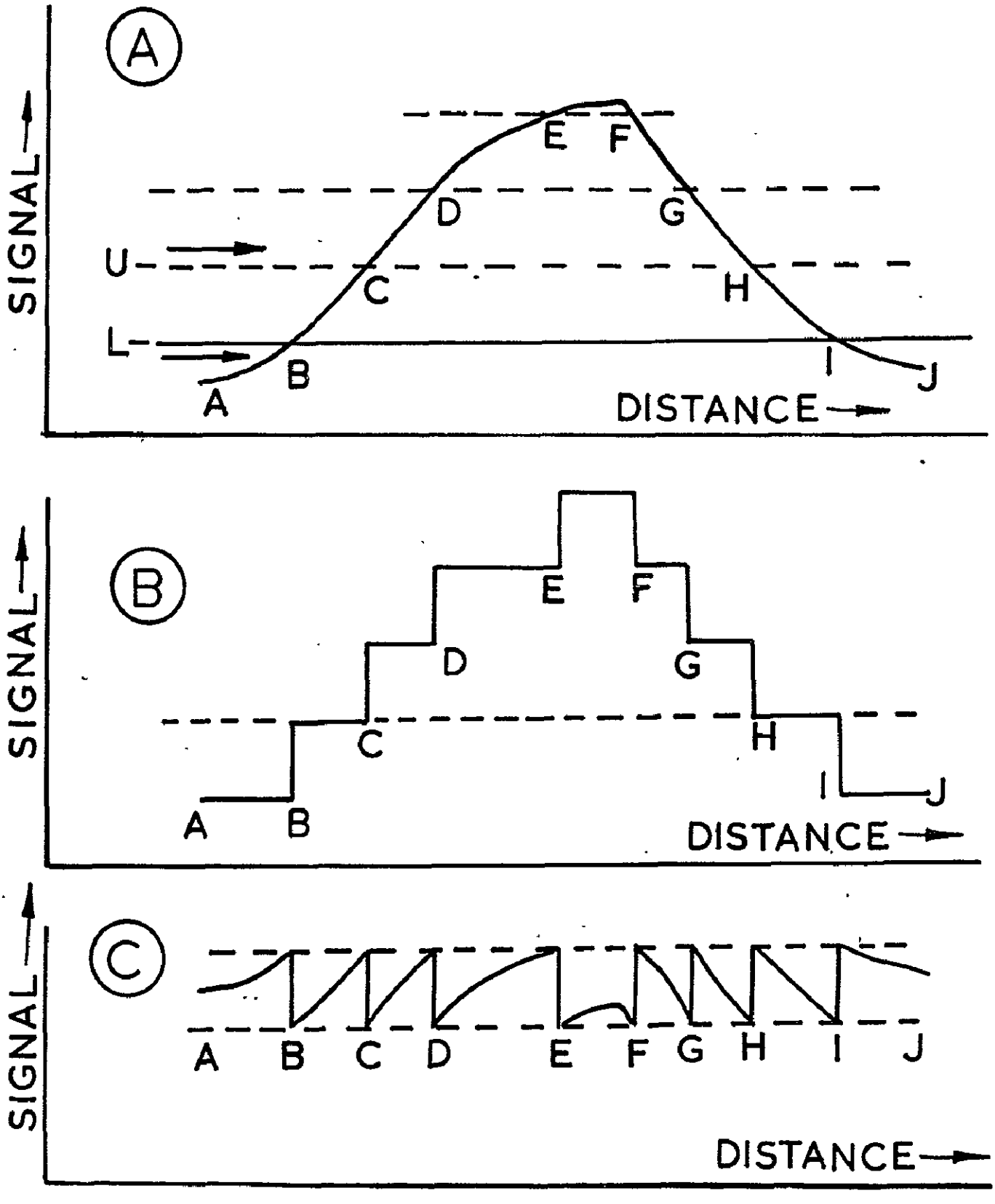
A
SIGNAL
U
L
A
B
C
D
E
F
G
H
I
J
DISTANCE
B
SIGNAL
A
B
C
D
E
F
G
H
I
J
DISTANCE
C
SIGNAL
A
B
C
D
E
F
G
H
I
J
DISTANCE

FIGURE. 2.

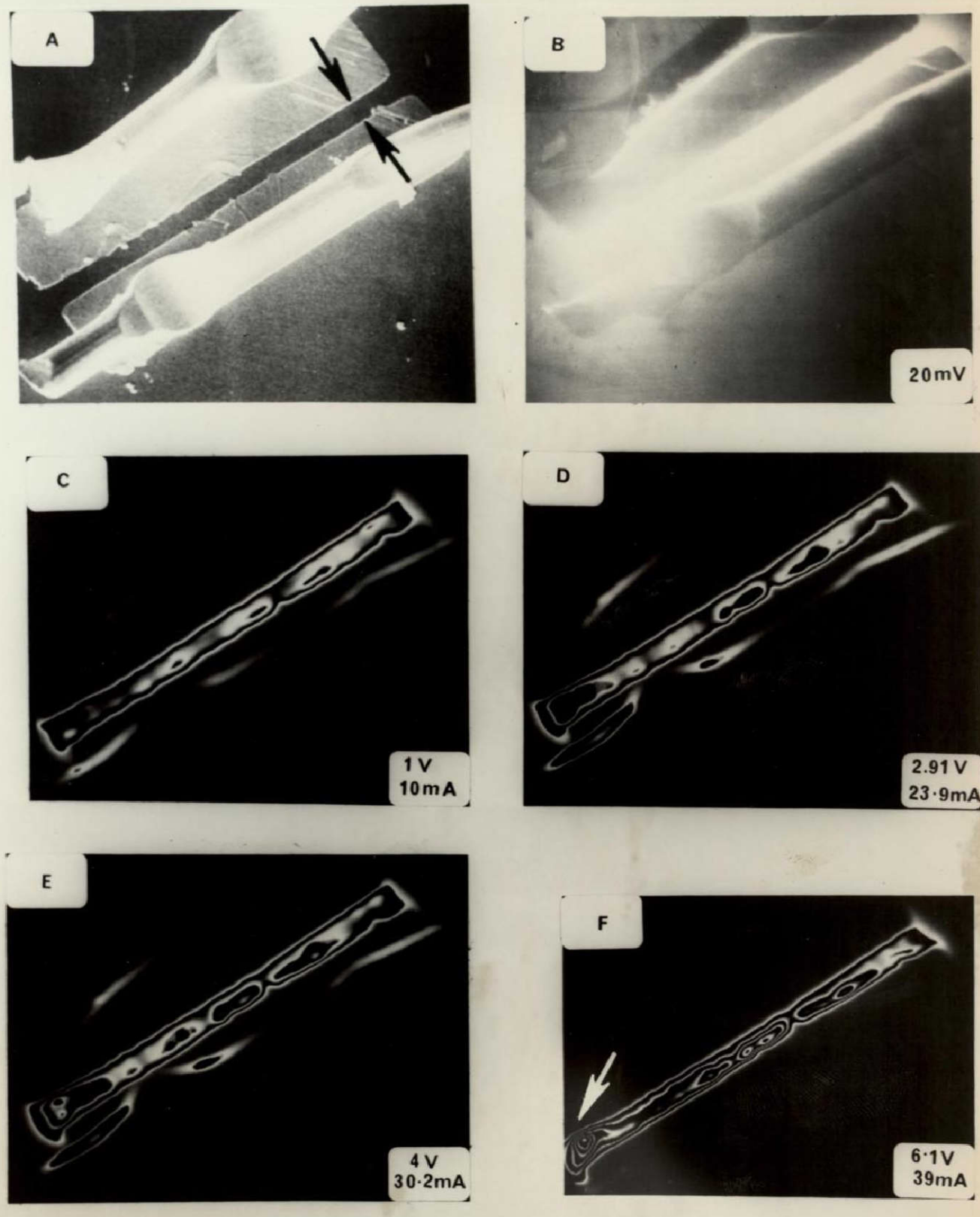

1.

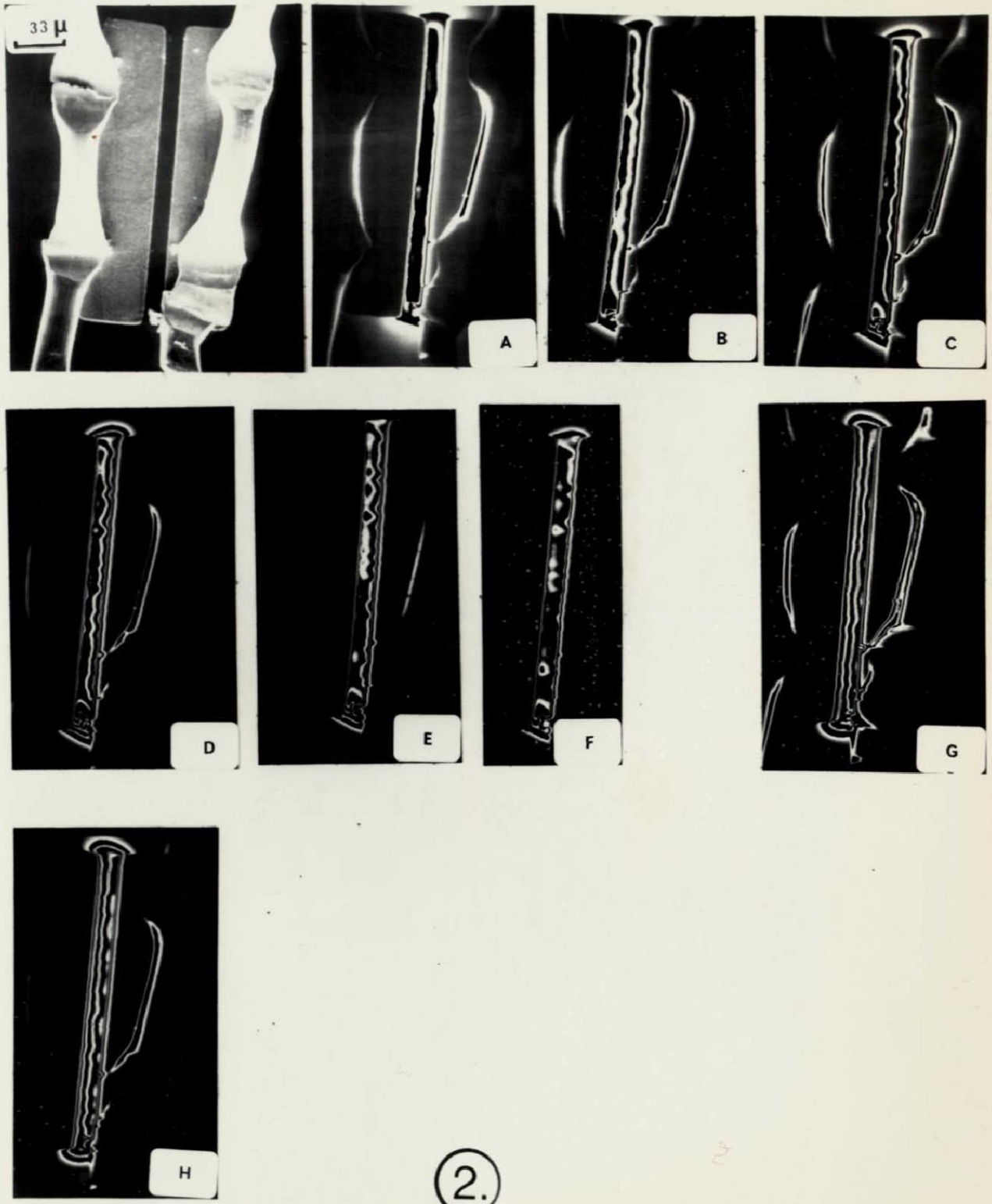
33 µ
A
B
C
D
E
F
G
H

3.

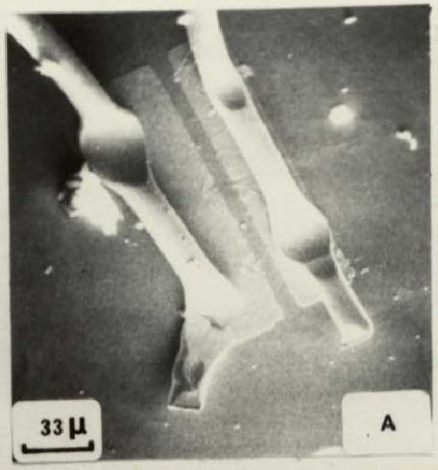

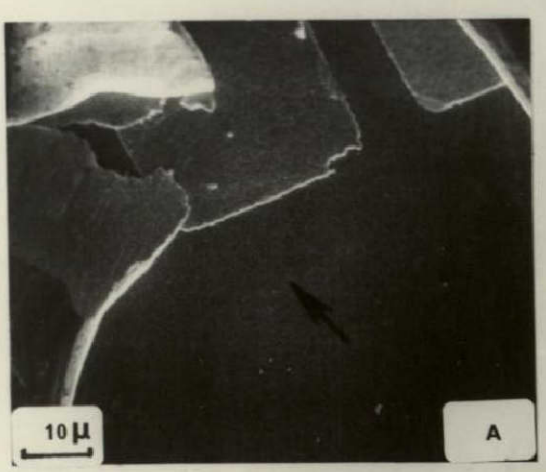

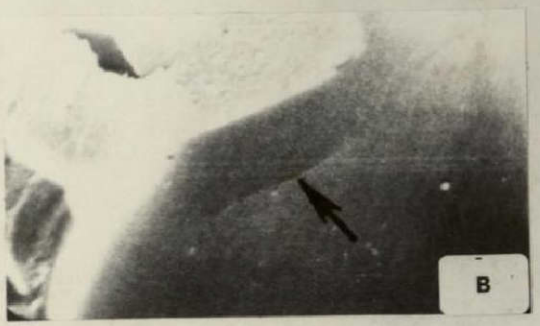

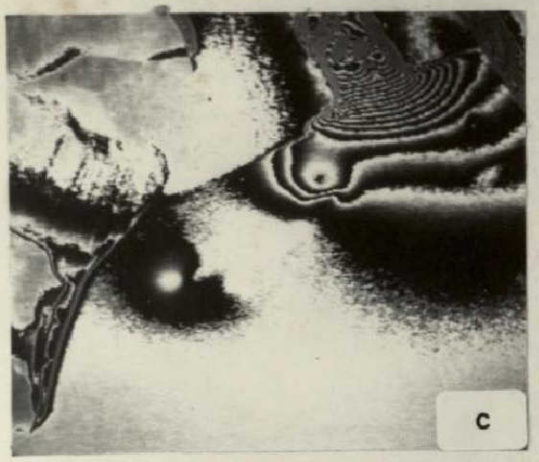

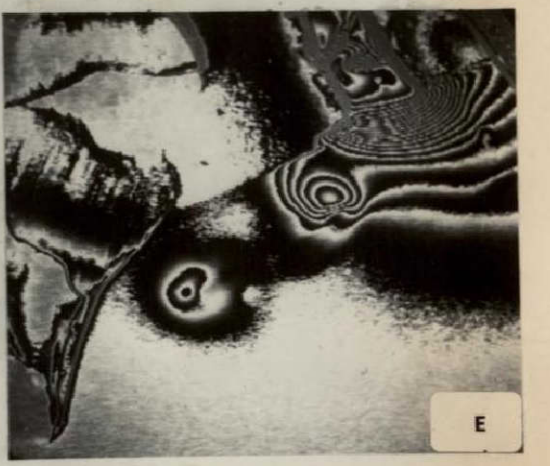

(4.)

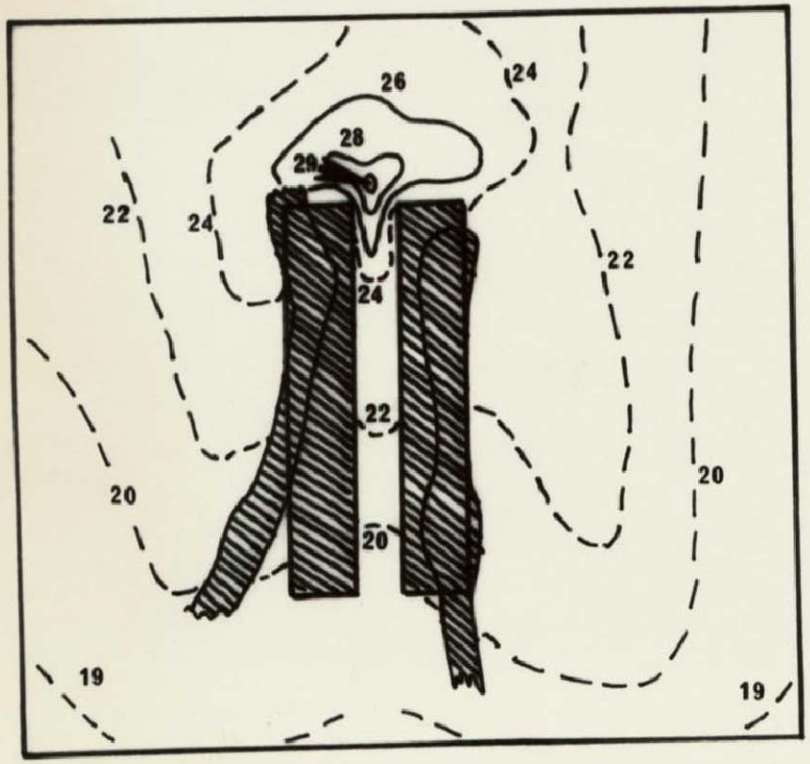
26
24
28
30
22
24
22
24
22
20
20
20
19
19

5.A.

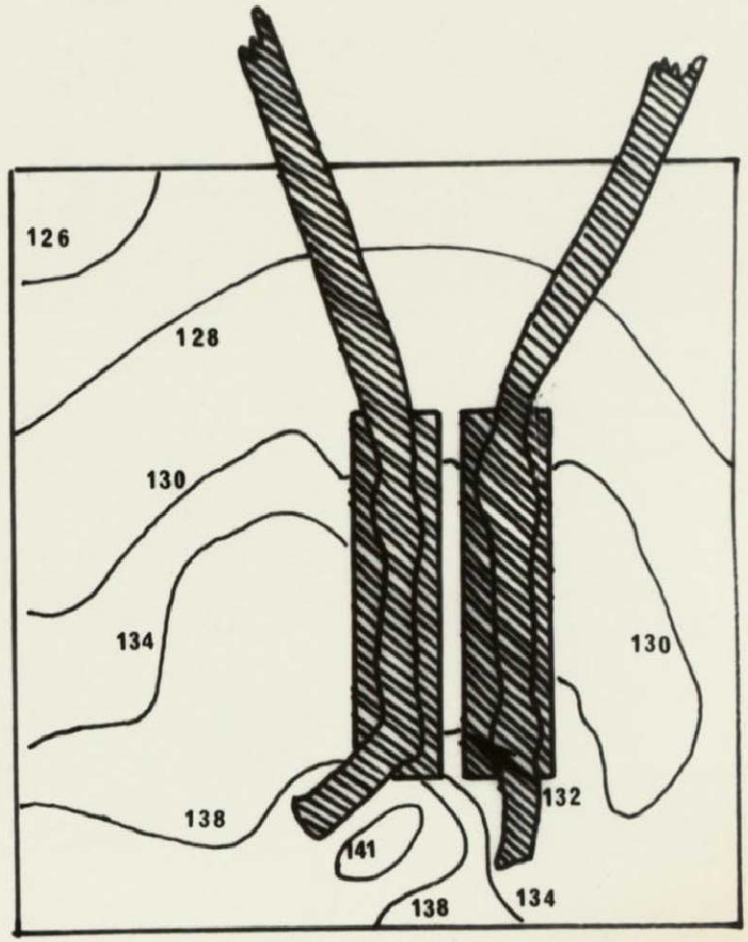
126
128
130
134
130
132
138
141
138
134

5.B.

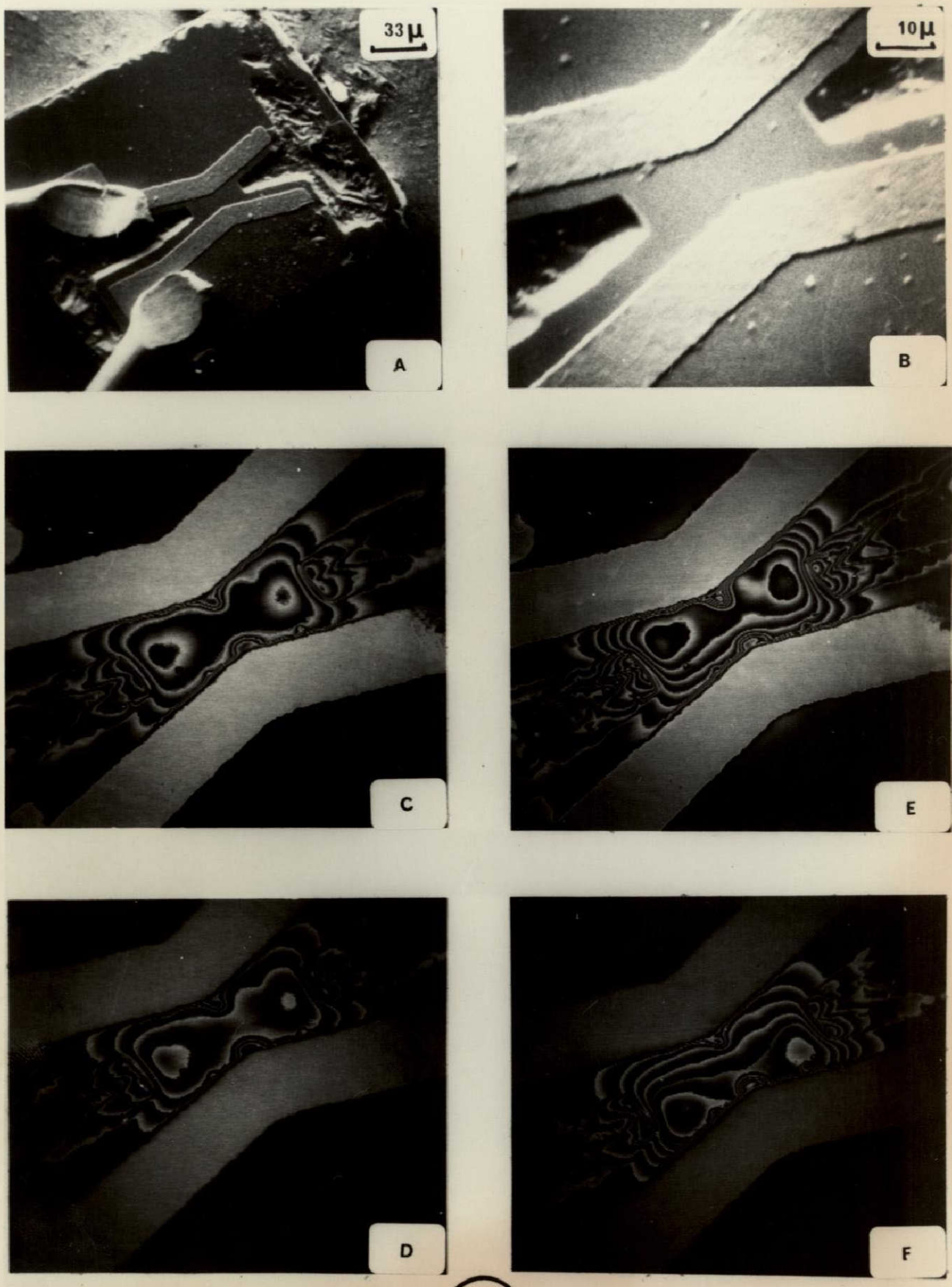

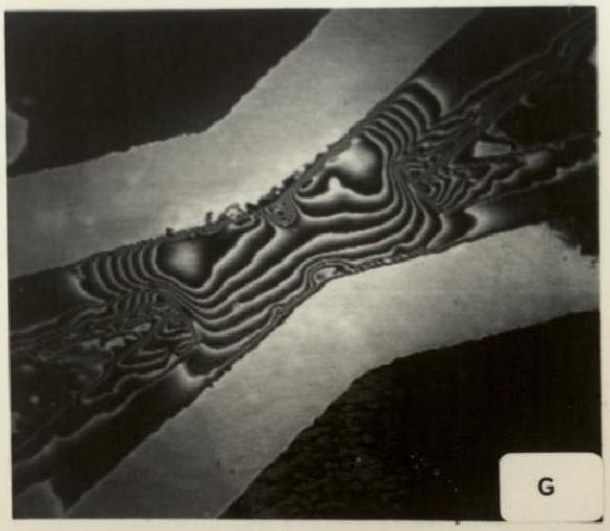

6.

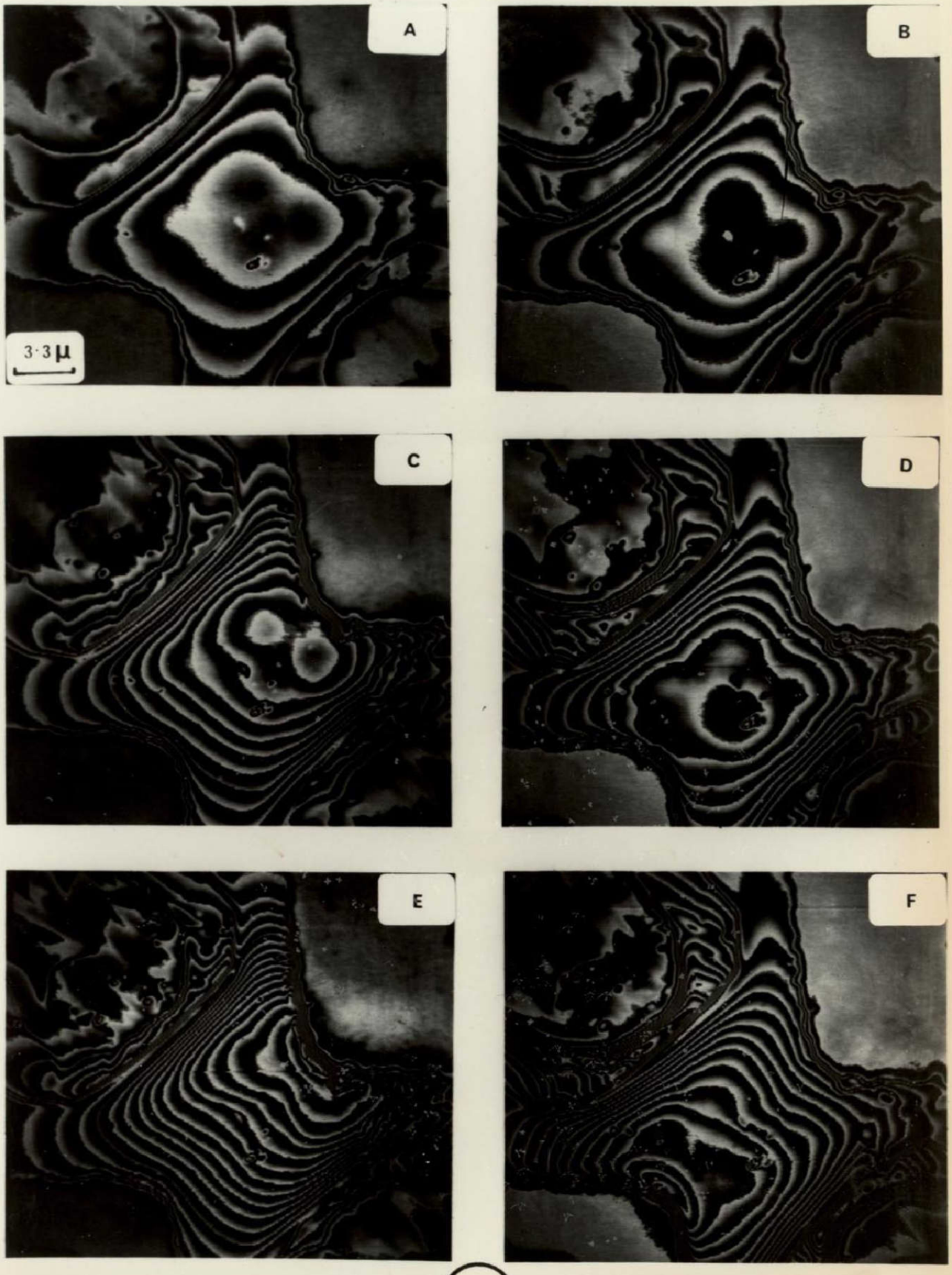
A
3·3 μ
B
C
D
E
F


G


H

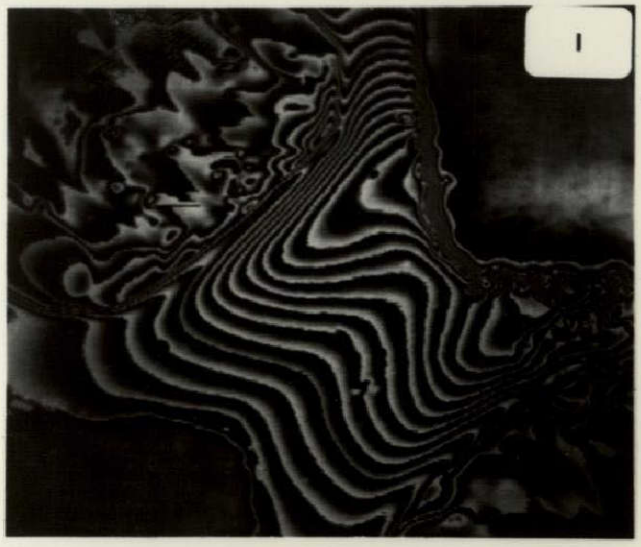
I

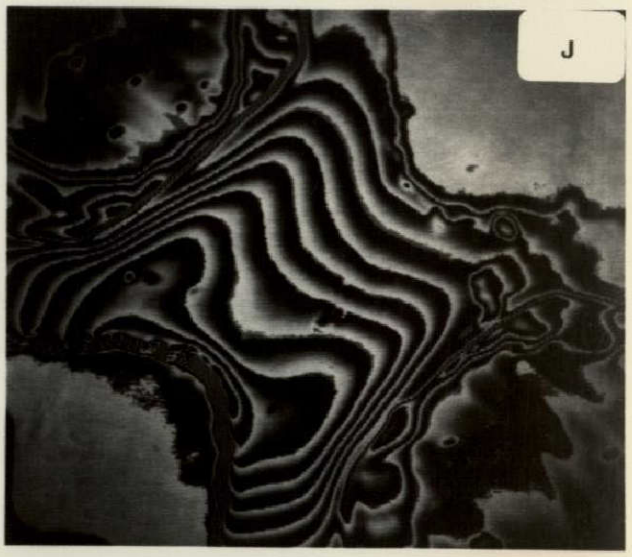
J


K


L

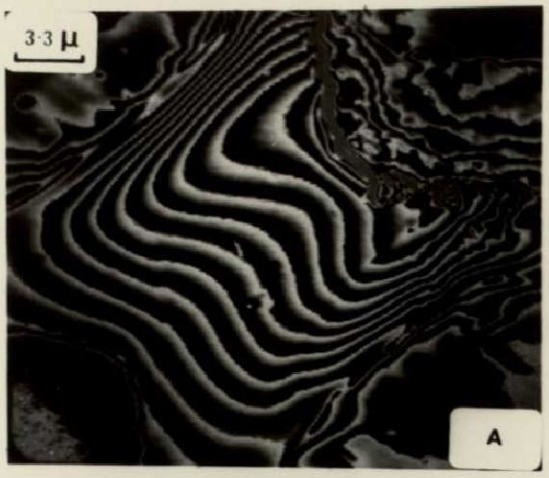
3·3 μ
A

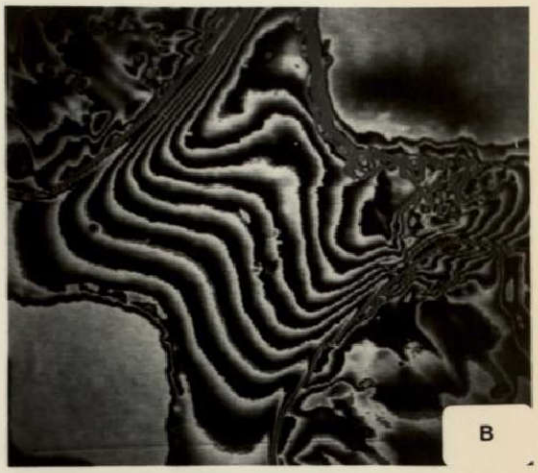
B


C


D


E

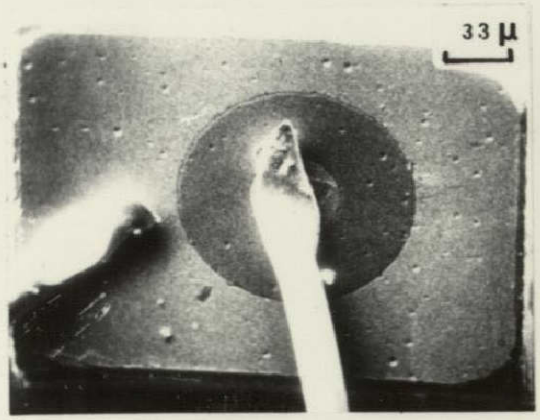

A

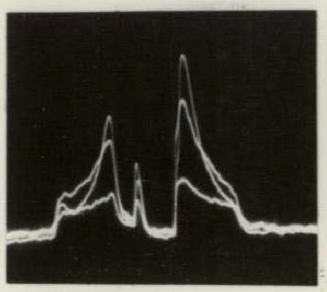

B

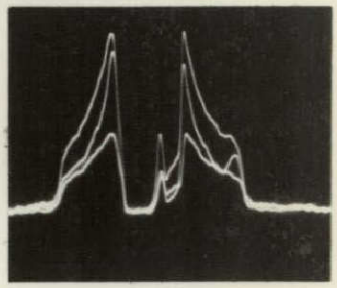

C

D

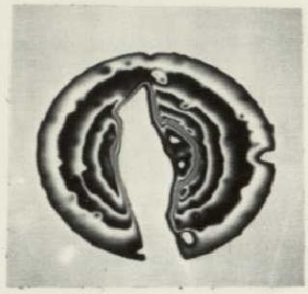

E

F

G

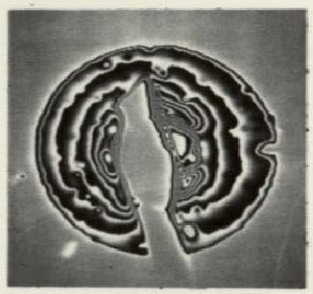

H

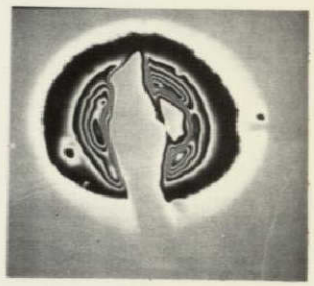

I

10.

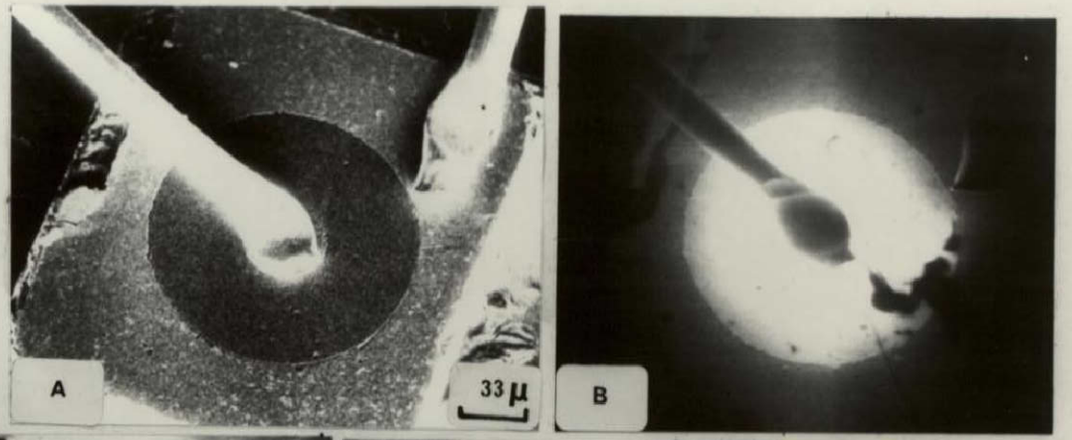

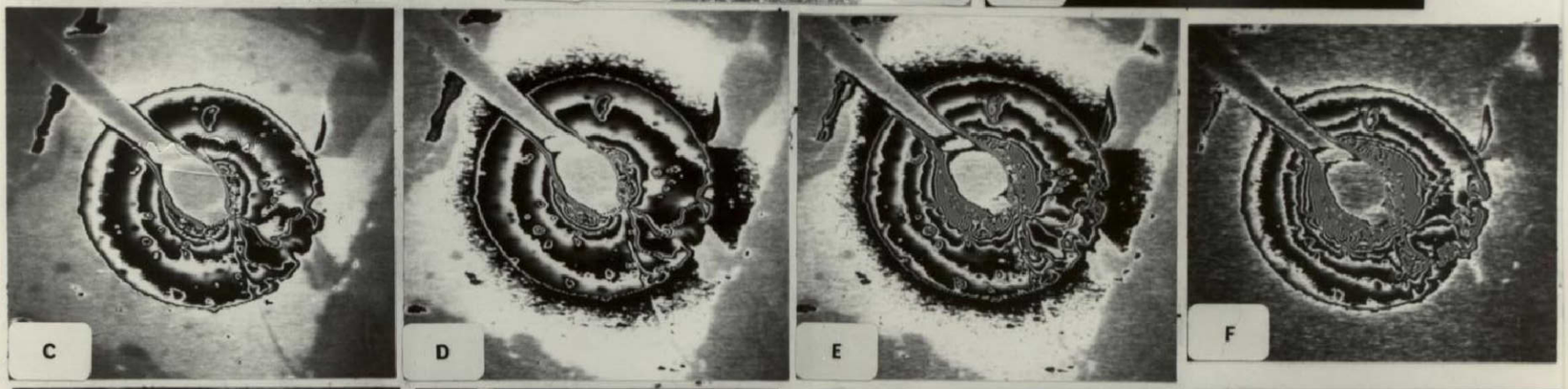

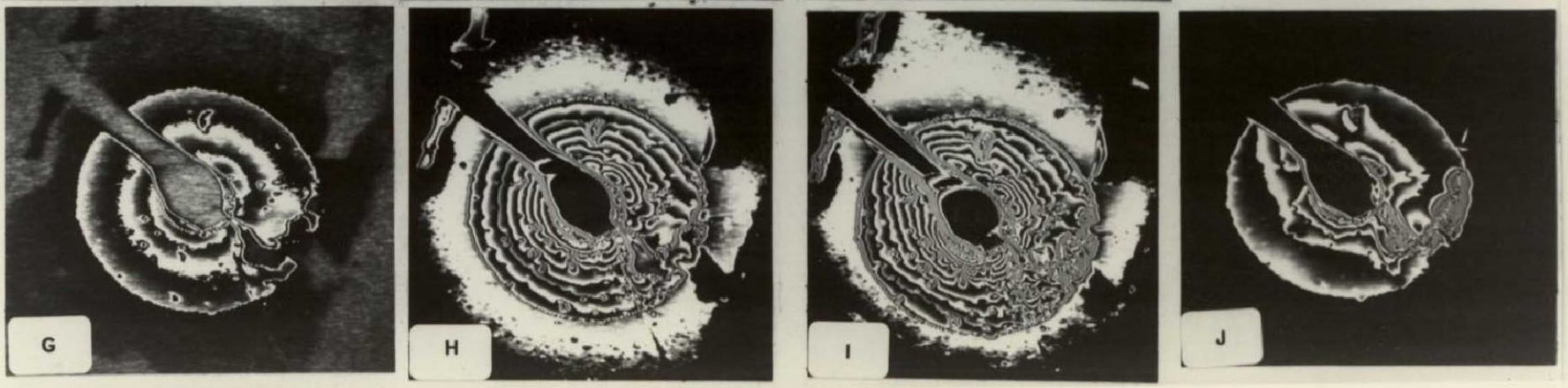

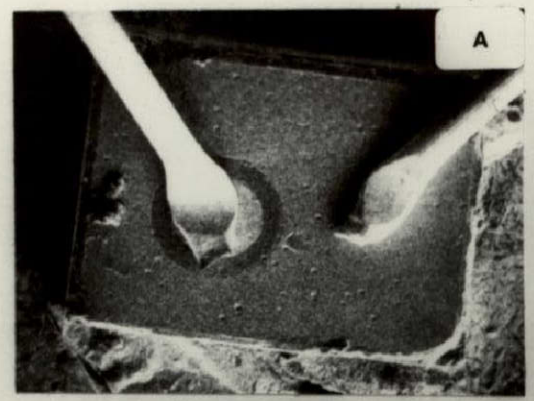

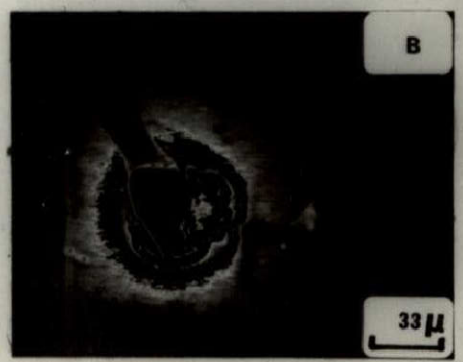

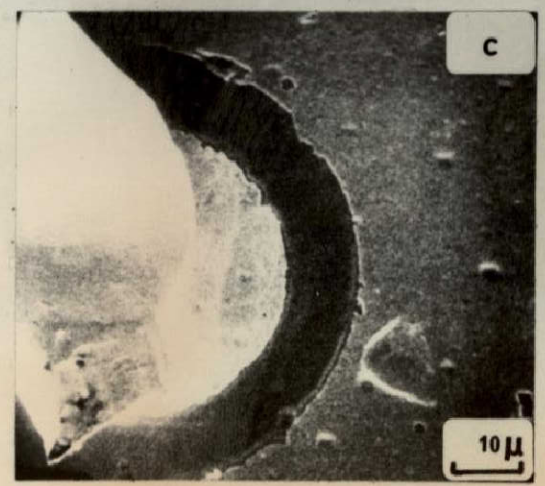

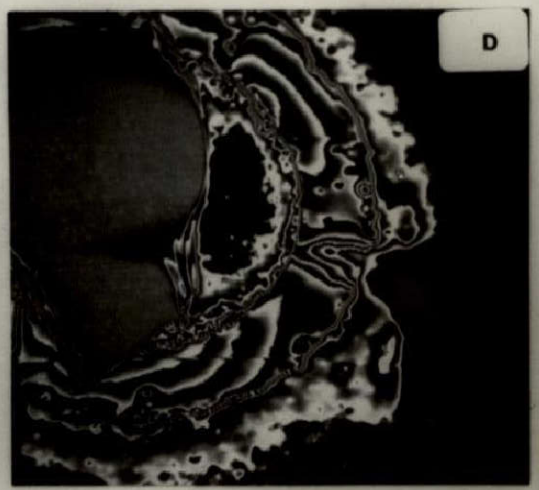

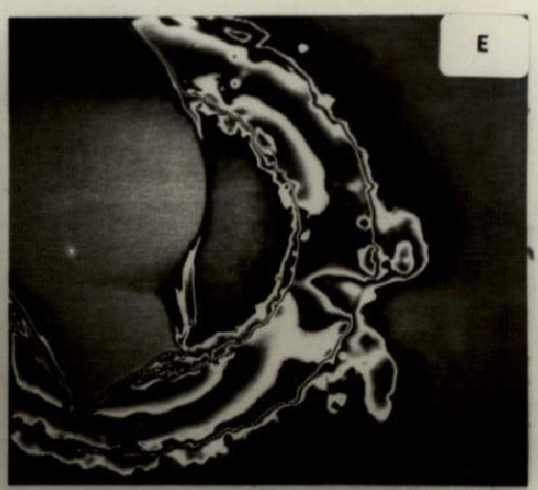

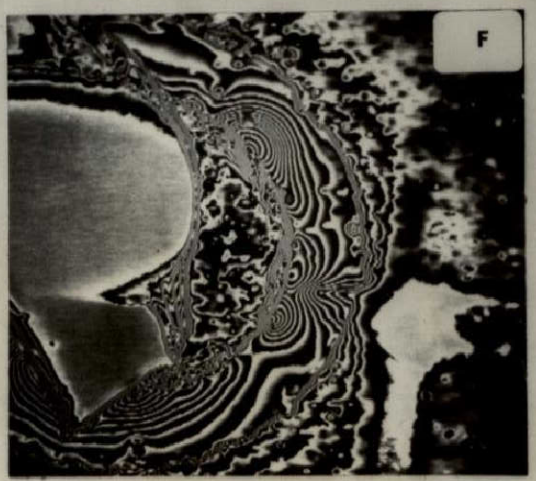

11.

12.

NOT REPRODUCIBLE

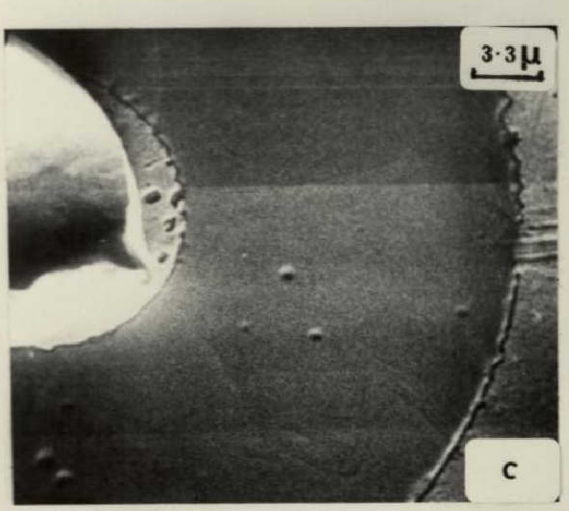

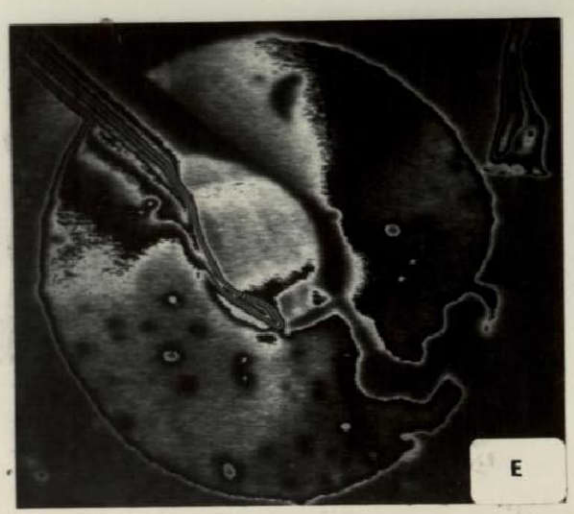

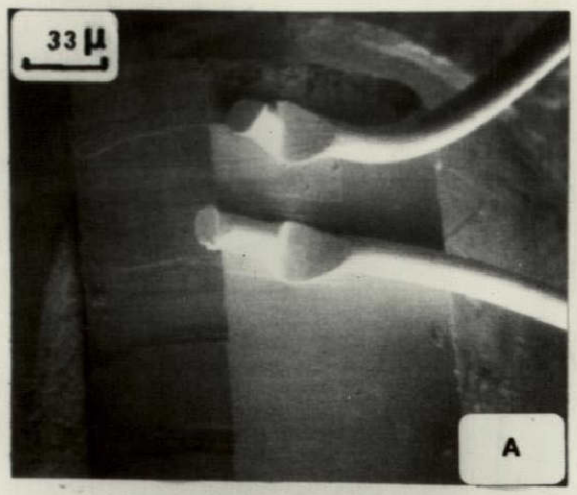

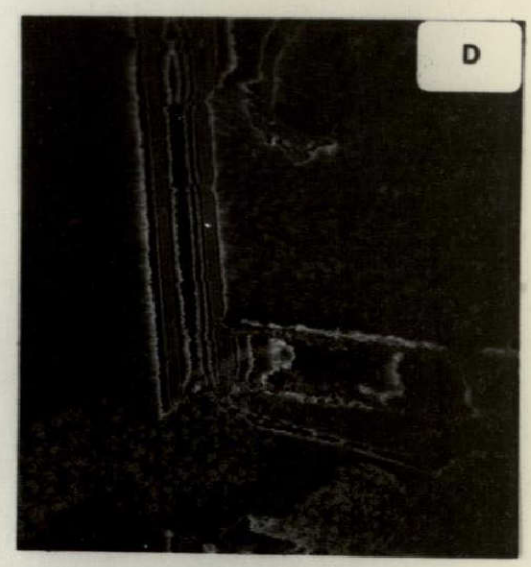

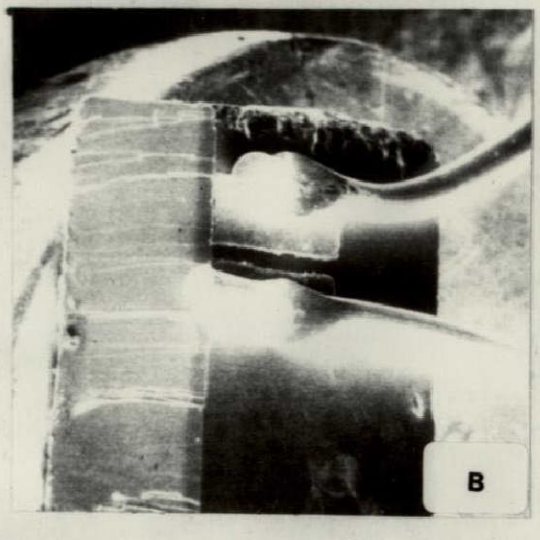

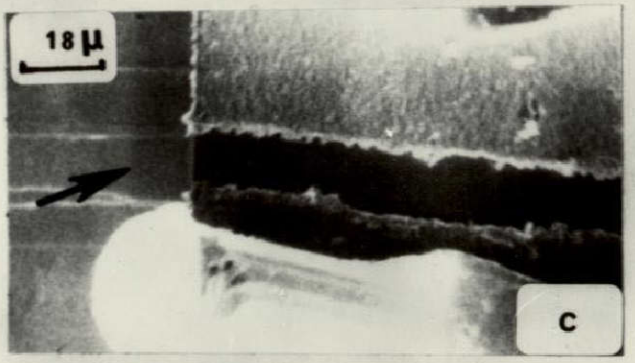

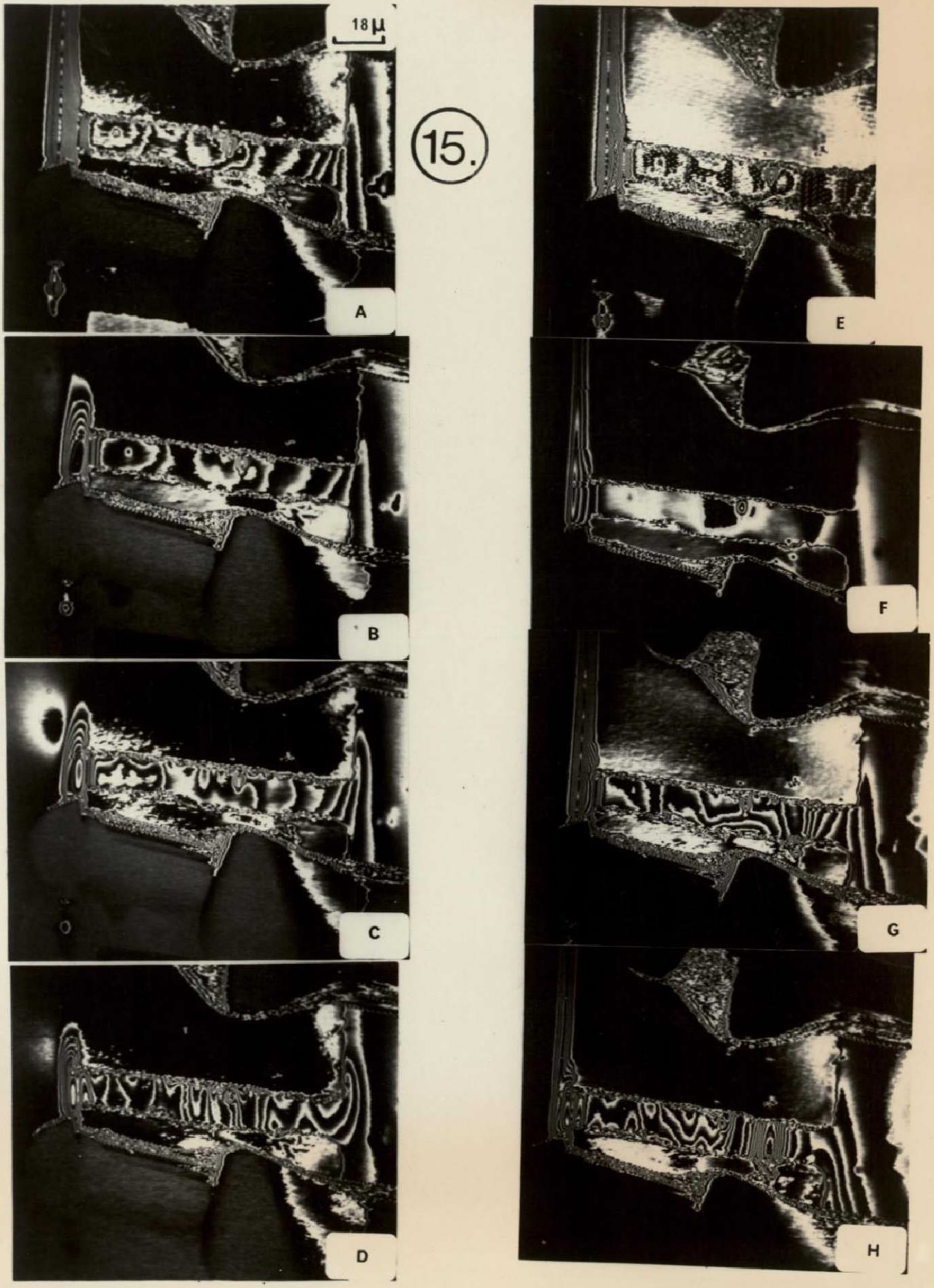

15.